学位申請論文

Three dimensional structure of ionospheric currents and the geomagnetic Sq field

竹田雅彦

論　文　内　容　の　要　旨

報告番号	甲第　　号	氏　名	竹田雅彦
論文調査担当者	主査　前田　坦 山元龍三郎　　國司秀明		

（論文題目）

Three dimensional structure of ionospheric currents and the geomagnetic Sq fields.

（電離層電流の3次元構造と地磁気Sq場）

（論文内容の要旨）

地磁気静穏日太陽日変化（Sq）を説明するものとして、電離層の風によるダイナモ理論が早くから知られている。そして、全地球的な電流系は電離層を薄い層とみなし、鉛直方向の電流を無視した「薄層ダイナモ」によって求められてきた。ただ、ロケット観測との比較のため、3次元構造が要請される赤道地方については、全地球的2次元計算から求められた電場分布を用いて、限られた地域での計算がなされている。しかし、このような方法では、全地球的な3次元電流構造が求まらないだけでなく、赤道地域と他の領域との間の電流のやりとりが無視されているため、正確な結果は期待できない。

申請者は、この問題を解決して全世界的な3次元電流系を求めるため、磁力線座標を用いることを思いついた。そして、磁力線方向の電気伝導度が垂直方向のそれに比べて非常に大きいことに注目してこれを無限大とみ

なし、3次元電流構造を2次元の式を解くことによって求める方法を考察した。

主論文の1部と2部においては、電離層内に存在するとされている、一日および半日周期の潮汐風によって作られる電流系を求めた。その結果、赤道地域では、今まで計算から予言され、観測で確かめられている子午面電流系が殆んど常に、どのモードの風についても存在し、電場の東西成分の向き、ジェット電流の発散、風の高度・緯度方向への変化などによって、その分布の様子がかなり変化することを見出した。そして、高さについて積分された電流系については、一日周期の風によるものが、地磁気Sq場から推定された等価電流系によく似ていることを確認した。これに対して、半日周期の風による電流系はそれとは似ていないので、このような風は平均的なSq場に寄与するよりも、赤道地方で時々みられる逆ジェット電流のような、Sq場の逐日変化に寄与しているものと考えた。そして実際、赤道逆ジェット電流が存在する場合の付加的な電流系は、半日周期風によるものとよく一致していることを示した。

現実の電離層では種々の原因、たとえば自転軸と磁軸のちがいや、季節による電気伝導度分布の変化などによって、電流分布は南北両半球で非対称になるものと思われる。申請者は3部において、このような場合に適用できるように計算方法を拡張し、その結果、Sq場のUT変化や季節変化を再現するとともに、南北両半球間での沿磁力線電流の構造をも明らかにした。

主論文の4部では、磁気圏起源の沿磁力線電流が、どのような電離層3次元電流系を作るかという問題を、電離層ダイナモの取扱い方法を応用することによって調べた。人工衛星の観測によると、磁気的に静かな時でもこのような沿磁力線電流が存在するので、申請者は観測に基づく沿磁力線電流分布と電気伝導分布とを用いて、電離層内での3次元電流系を求めた。その結果、このような場合にも子午面電流系が形成されるが、電流強度は

主論文

THREE DIMENSIONAL STRUCTURE OF IONOSPHERIC CURRENTS AND THE GEOMAGNETIC SQ FIELD

MASAHIKO TAKEDA

ABSTRACT

We present a new method to calculate three dimensional ionospheric currents using magnetic field line coordinate system and the assumption of infinite parallel conductivity. Then we calculate ionospheric currents by tidal winds and find that meridional current system in the equatorial region almost always exists, only changing its form according to sources and local time. Diurnal tidal winds produce current system similar to that deduced from geomagnetic solar quiet daily variation (Sq). Current by semidiurnal winds is dissimilar to it, but may explain day-to-day variation of Sq such as the equatorial counter electrojet. Next we examine the effect of asymmetry with respect to the equator and succeed in reproduction of the UT variation of Sq and field-aligned currents generated by ionospheric dynamo action. Effects of field-aligned currents originated in the magnetosphere are also studied under geomagnetically quiet condition and it is found that they are important to day-to-day variation of Sq only at high latitudes but ineffective to that at low latitudes.

CONTENTS

1. INTRODUCTION

The regular daily variation in geomagnetic field (Sq), which was first discovered by Graham (1722), has been studied by many workers. Baker (1953) and Van Sabben (1962) developed the thin shell dynamo model which assumes no vertical current, and Tarpley (1970a, b) showed that tidal winds of (1,-2) mode mainly contribute to Sq using this model. This conclusion is confirmed by Forbes and Lindzen (1976a) and Richmond et al. (1976). However, as thin shell model assumes that the electrostatic potential does not change with altitude, and that the vertical current is neglegible, it is inadequate to calculate three dimensional current especially near the equator. Stening (1968, 1969) calculated global ionospheric current system by an equivalent circuit method, but because of a lower boundary condition of no parallel current, he failed to reproduce the currents near the equator.

On the other hand, Bartels and Johnston (1940) found that Sq at the equatorial station has large amplitude. Egedal (1948) presented the idea that the enhancement of geomagnetic variation is caused by an enhanced east-west overhead current, and this current is called "equatorial electrojet". Sugiura and Cain (1966) presented a model using the assumption of no vertical current, which is the same as in the thin shell model. However, Untiedt (1967) and Sugiura and Poros (1969) pointed out that a self-consistent model must allow for some vertical current, and they calculated three dimensional

currents in the meridional plane, ignoring longitudinal derivatives. Richmond (1973a, b) used orthogonal magnetic coordinate to study the equatorial electrojet and showed that infinite parallel conductivity ($\sigma_0 = \infty$) model is fairly good. These calculations are made in the meridional plane, and assume that the longitudial extent of the equatorial electrojet is so large in comparison with its width that longitudinal gradients of electric fields, conductivities and currents can be neglected. Gagnepain et al. (1976), however, evaluated the effects of them in the equatorial electrojet and showed that the gradients may cause qualitative variation of vertical structure. Forbes and Lindzen (1976b) studied a three dimensional model by using values calculated from a global thin shell model (Forbes and Lindzen, 1976a) as boundary condition. These previous workers, however, calculated global potential distribution and three dimensional structure of the equatorial electrojet separately, and therefore these calculations are not globally self-consistent.

In this paper, we first present a method by which three dimensional currents at any point are obtained self-consistently, using the assumption of infinite parallel conductivity ($\sigma_0 = \infty$), and calculate three dimensional currents generated by tidal winds of diurnal (1,-2) and semidiurnal (2,2) and (2,4) modes, and by field-aligned currents of magnetospheric origin. Then we discuss their contribution to Sq including the equatorial electrojet, and its day-to-day variation, such as the equatorial counter electrojet which was found by Bartels and Johnston (1940). Ionospheric currents and field-aligned currents generated by ionospheric dynamo asymmetrical with respect to the equator are also examined.

2. FORMULATION OF THE PROBLEM

Ionosphere is consist of magnetized plasma, and so it is natural to take coordinate referring to the magnetic field line for the calculation of electric fields and currents in the ionosphere. Stening (1968) used this feature by representing the ionosphere as sum of blocks, each of which comprises a whole tube of magnetic force, and by calculating the ionospheric currents using his equivalent circuit method. Richmond (1973a, b) applied coordinate referring to the magnetic field to simulate the equatorial electrojet in the meridional plane and found that parallel conductivity (σ_0) may be put infinite. Here, we first represent three dimensional equation $\nabla\cdot\mathbf{j} = 0$, using orthogonal magnetic coordinates (t,s,ϕ), such as:

$$t = \frac{r_0 \sin^2\theta}{r}, \quad s = \frac{r_0^2 \cos\theta}{r^2}, \quad \phi = \phi \tag{1}$$

where θ is the geomagnetic colatitude, ϕ is the longitude, r is the geocentric distance, and r_0 is that of the lower boundary of the ionosphere. Here, we have assumed a dipole magnetic field and a spherical earth. The geometrical scale factors are then given by

$$h_t = \frac{r^2}{r_0 \sin\theta \sqrt{1+3\cos^2\theta}}, \quad h_s = \frac{r^3}{r_0^2 \sqrt{1+3\cos^2\theta}}, \quad h_\phi = r\sin\theta \tag{2}$$

Using this coordinate system, the equation $\nabla\cdot\mathbf{j} = 0$ gives

$$\frac{\partial(h_s h_\phi j_t)}{\partial t} + h_t h_s \frac{\partial j_\phi}{\partial \phi} = -\frac{\partial}{\partial s}(h_\phi h_t j_s) \tag{3}$$

Three components of electric current (j_t, j_s, and j_ϕ) are expressed by the electrostatic potential S, the horizontal southward (u) and eastward (v) wind velocities, the total geomagnetic field B, the vertical upward component of it B_r, and the parallel, Pedersen, and Hall conductivities σ_0, σ_1, and σ_2 as follows:

$$j_t = \sigma_1 \left(-\frac{1}{h_t}\frac{\partial S}{\partial t} - vB \right) + \sigma_2 \left(-\frac{1}{h_\phi}\frac{\partial S}{\partial \phi} - uB_r \right) \tag{4}$$

$$j_s = \sigma_0 \left(-\frac{1}{h_s}\frac{\partial S}{\partial s} \right) \tag{5}$$

$$j_\phi = -\sigma_2 \left(-\frac{1}{h_t}\frac{\partial S}{\partial t} - vB \right) + \sigma_1 \left(-\frac{1}{h_\phi}\frac{\partial S}{\partial \phi} - uB_r \right) \tag{6}$$

Substituting equations (4) and (6) into equation (3), we obtain

$$a\frac{\partial^2 S}{\partial t^2} + b\frac{\partial^2 S}{\partial \phi^2} + d\frac{\partial S}{\partial t} + e\frac{\partial S}{\partial \phi} + f = -\frac{\partial}{\partial s}(h_\phi h_t j_s) \tag{7}$$

where

$$a = \frac{h_s h_\phi \sigma_1}{h_t}, \quad b = \frac{h_t h_s \sigma_1}{h_\phi}, \quad d = -\frac{\partial}{\partial t}\left(\frac{h_s h_\phi}{h_t}\sigma_1\right) + h_s\frac{\partial \sigma_2}{\partial \phi},$$

$$e = -\frac{\partial}{\partial t}(h_s\sigma_2) - \frac{h_t h_s}{h_\phi}\frac{\partial \sigma_1}{\partial \phi},$$

$$f = -\frac{\partial}{\partial t}(h_s h_\phi(\sigma_1 vB + \sigma_2 uB_r)) - \frac{\partial}{\partial \phi}(h_t h_s(\sigma_1 uB_r - \sigma_2 vB))$$

Equation (7) is an exact expression and if we substitute equation (5) into equation (7), we obtain complete three dimensional equation. Three dimensional equation is, however, generally difficult to solve and especially difficult in this case, where anisotropy of conductivity that σ_0 is much greater than σ_1 and σ_2, may be apt to cause numerical instability. Therefore we make use of the fact that σ_0 is large, and use infinite parallel conductivity model ($\sigma_0 = \infty$). Then derivative of S along magnetic field line becomes zero everywhere, and so $\frac{\partial^2 S}{\partial t^2}$, $\frac{\partial^2 S}{\partial \phi^2}$, $\frac{\partial S}{\partial t}$, and $\frac{\partial S}{\partial \phi}$ are constant on it. Therefore when we integrate equation (7) along magnetic field line, it becomes possible to integrate the coefficients (a,b,d,e,f) only. Then the result is as follows:

$$A\frac{\partial^2 S}{\partial t^2} + B\frac{\partial^2 S}{\partial \phi^2} + D\frac{\partial S}{\partial t} + E\frac{\partial S}{\partial \phi} + F = [\, - h_\phi h_t j_s]_{s_1}^{s_2} \qquad (8)$$

where $A = \int_{s_1}^{s_2} a\, ds$, etc. and s_1 and s_2 are values of s at lower and upper boundary, respectively. Values of j_s at $s=s_1$ and s_2 are determined from boundary conditions. Lower boundary condition we use here is that the vertical current $j_r = 0$, because vertical gradient of conductivity at the lower boundary is so large that currents are confined above the boundary. As j_r is expressed as

$$j_r = j_s \sin I + j_t \cos I \qquad (9)$$

where I is the dip angle, j_s becomes as

$$j_s = - j_t \cot I$$

$$= \frac{\tan\theta}{2} \left(\frac{\sigma_1}{h_t} \frac{\partial S}{\partial t} + \frac{\sigma_2}{h_\phi} \frac{\partial S}{\partial \phi} + (\sigma_1 v B + \sigma_2 u B_r) \right) \tag{10}$$

Substituting equation (10) at $s=s_1$, we obtain the following equation

$$A \frac{\partial^2 S}{\partial t^2} + B \frac{\partial^2 S}{\partial \phi^2} + D' \frac{\partial S}{\partial t} + E' \frac{\partial S}{\partial \phi} + F' = - (h_t h_\phi j_s)_{s=s_2} \tag{11}$$

where

$$D' = D + \left(\frac{\sigma_1 h_\phi \tan\theta}{2} \right)_{s=s_1}, \quad E' = E + \left(\frac{\sigma_2 h_t \tan\theta}{2} \right)_{s=s_1},$$

$$F' = F + \left(\frac{(\sigma_1 v B + \sigma_2 u B_r) \tan\theta}{2} \right)_{s=s_1}$$

Substituting proper values for j_s at $s=s_2$, we solve equation (11) by a relaxation method using a boundary condition $j_r = j_t = 0$ at the lower boundary of the equatorial ionosphere. Once we get $S(t,\phi)$, j_t and j_s are calculated from equations (4) and (6). As we assume $\sigma_0 = \infty$, j_s is obtained not from equation (5) but by integration of equation (7).

In the following calculations we use a three dimensional conductivity model, which is partly shown in Figs. 1-3, from 90 to 400 km. Mesh points are at every 7.5° (half an hour) along the longitude, and there are 85 points with t, the intervals of which expressed by t are small near the pole, large at midlatitude, and very small near the equator. Integration of equation (7) is performed by using values at every 5 km height from 90 to 200 km and every 25 km from 200 to 400 km.

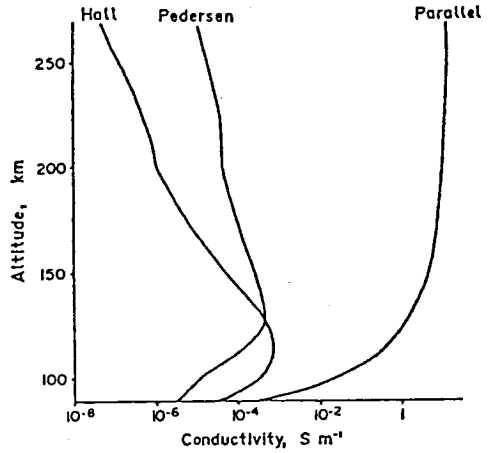

Fig. 1. Conductivity profile at the equator at noon.

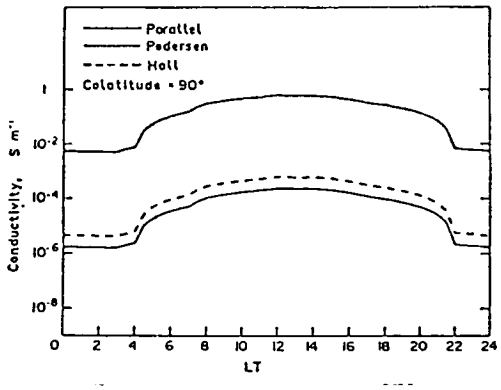

Fig. 2. The daily variation of conductivities at an altitude of 120 km at the equator.

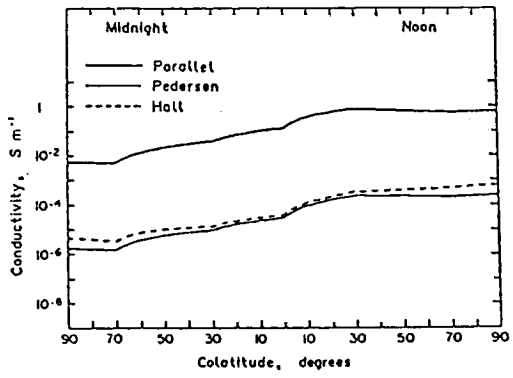

Fig. 3. Latitudinal profile of conductivities at an altitude of 120 km along the noon-midnight meridian.

3. CALCULATION FOR SYMMETRICAL TIDAL WINDS

When we calculate under the condition that parameters, such as conductivities, winds and geomagnetic field, are all symmetrical with respect to the equator, we can put $j_s = 0$ at $s=s_2$. At the equinox, this assumption may be justified if we ignore difference between geographic and geomagnetic coordinates, and assume dipole magnetic field. Asymmetrical cases are discussed in the next chapter. Wind model used here is that presented by Salah and Evans (1977), which is shown in Fig. 4. This model gives tidal winds of (1,-2), (2,2) and (2,4) modes from 90 to 200 km in altitude. We calculate currents for these three modes individually, assuming that the winds above 200 km have the same amplitude and phase with those at 200 km.

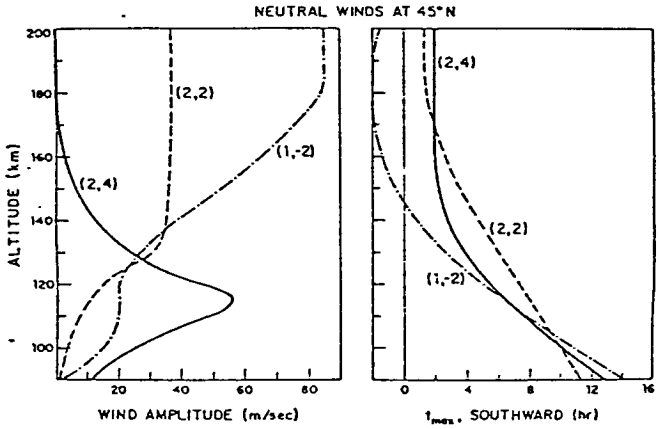

Fig. 4. Tidal winds shown by Salah and Evans (1977).

3-1. CURRENTS CAUSED BY DIURNAL TIDAL WINDS

Electrostatic potential distribution at 90 km by (1,-2) mode tidal winds is shown in Fig. 5 and height integrated horizontal currents in the E (90-150 km) (top) and F (150-400 km)

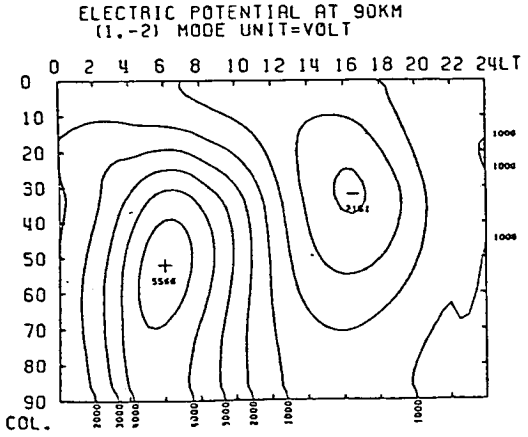

Fig. 5. Electrostatic potential at 90 km. Contours are drawn at every 1000 V.

(middle) layers, and in the total ionosphere (bottom) are given in Fig. 6. This total current system is essentially consistent with the observed Sq current system (e.g. Matsushita and Maeda, 1965; Malin, 1973) and results calculated by using the thin shell model (Tarpley, 1970b; Richmond et al., 1976). Currents mainly flow in E layer, but F layer currents are not negligible especially at middle and high latitudes and contribute to the poleward current in the afternoon about as much as E layer currents.

Figures 7-10 show eastward current densities (bottom) and currents in a meridional plane (top) in the equatorial region at 0000, 0600, 1200 and 1800 LT, respectively. Figure 11 gives two components of the electric field normal to magnetic field lines and their contribution to eastward electric currents at 100 km in the equatorial region at 1200 LT (left) and 1800 LT (right). The current system in the meridional plane at noon is similar to that predicted by Untiedt (1967)

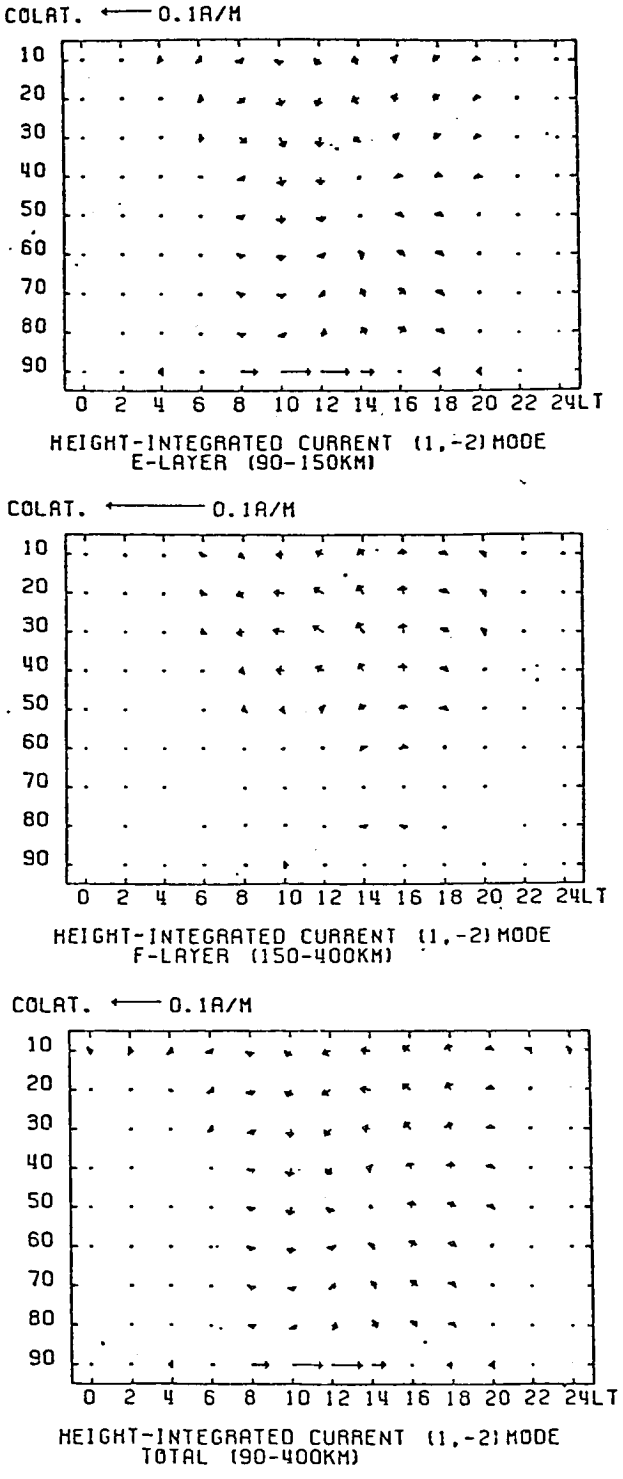

Fig. 6. Height-integrated current distribution in (θ,ϕ) plane in the E layer (top), F layer (middle), and total ionosphere (bottom).

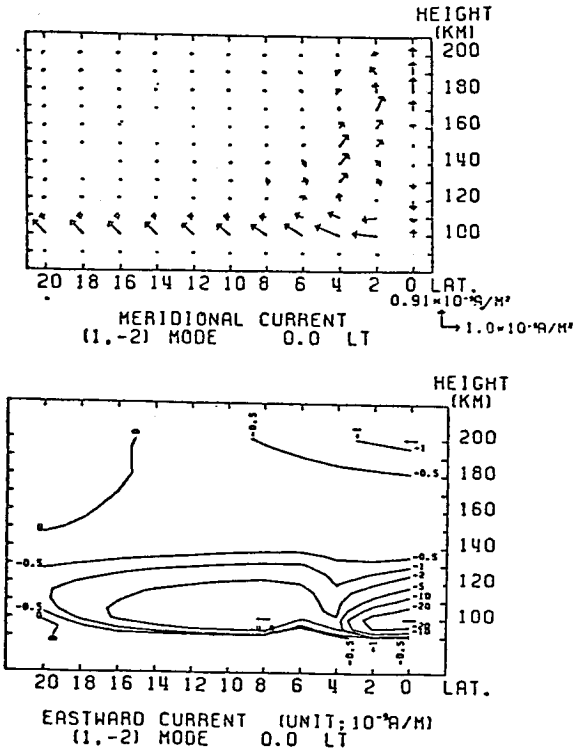

Fig. 7. Meridional current structure (top) and eastward current density (bottom) between 0° and 20° in latitude at 0000 LT.

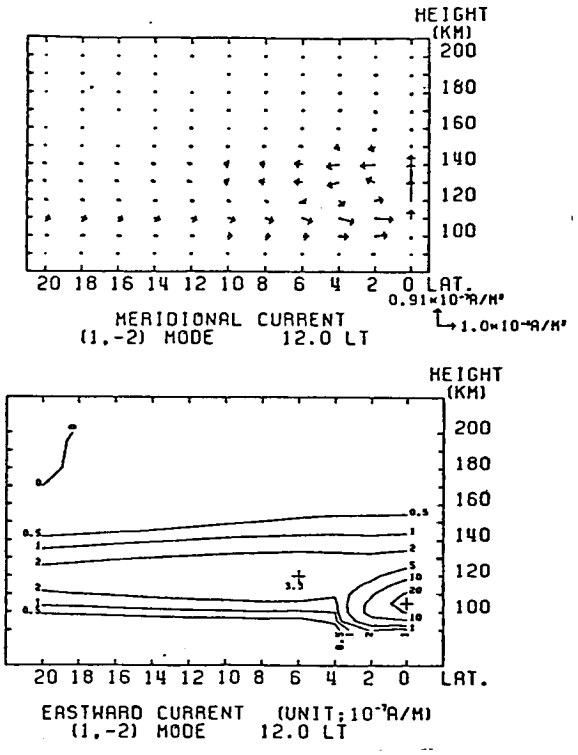

Fig. 9. Same as in Fig. 7 but at 1200 LT

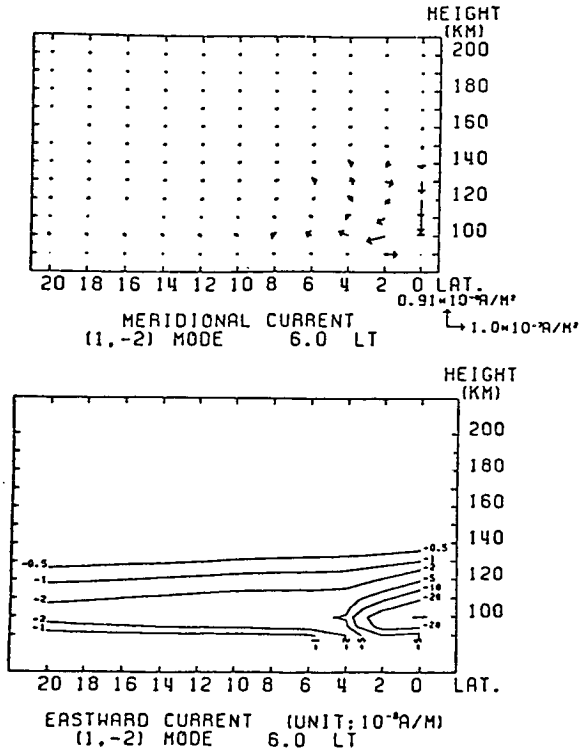

Fig. 8. Same as in Fig. 7 but at 0600 LT.

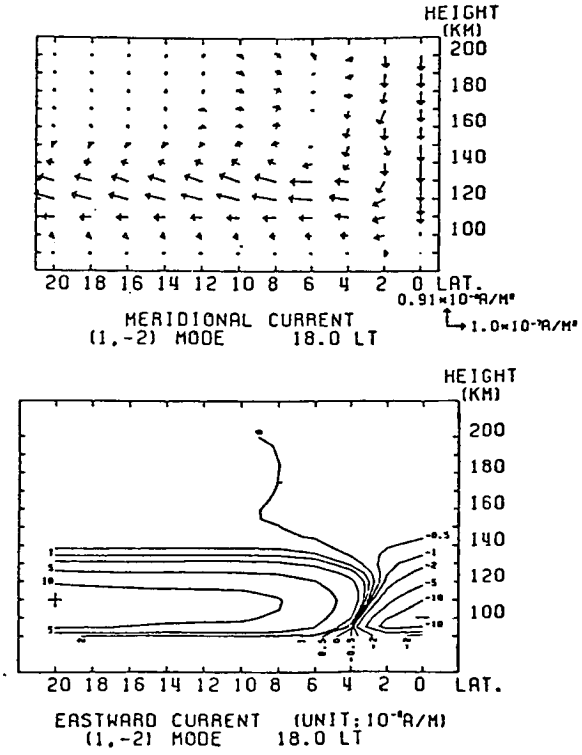

Fig. 10. Same as in Fig. 7 but at 1800 LT.

and observed by Musmann and Seiler (1978). This system also appears in about the same manner at 0600 LT. At 0000 and 1800 LT this system is reversed because the east-west component of electric field is reversed. At 1800 LT a strong poleward current flows at about 125 km and is not compensated by equatorward current at other altitudes, forming height integrated poleward currents. On the other hand, equatorward current flows mainly at lower altitudes (110 km) in the morning. These show that the meridional current system itself always exists, only changing its direction according to the sign of east-west component of electric field, and the equatorward and poleward current parts are enhanced in the morning and afternoon, respectively, and the other parts are diminished.

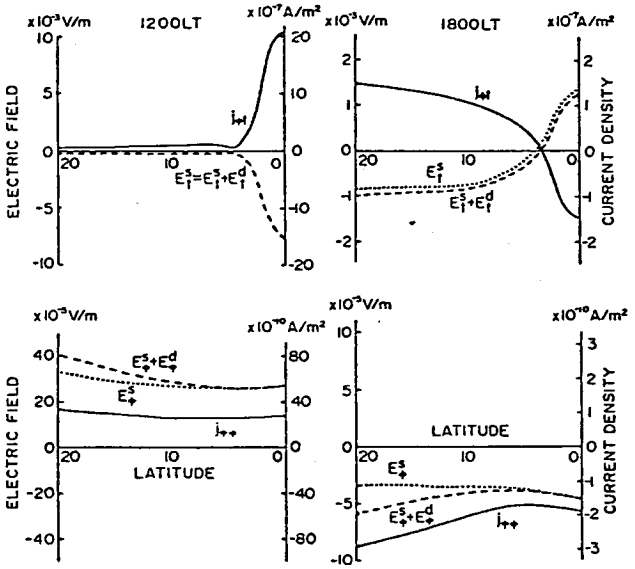

Fig. 11. Electric fields (E_t^s, E_t^d, E_ϕ^s, and E_ϕ^d) and their contribution to eastward currents ($j_{\phi t}$ and $j_{\phi\phi}$) at 1200 LT (left) and 1800 LT (right). Superscripts s and ϕ refer to the direction of the principal normal and binormal of magnetic field lines, respectively. The $j_{\phi t}$ is the current density driven by $E_t^s + E_t^d$, and $j_{\phi\phi}$ by $E_\phi^s + E_\phi^d$.

At noon it is clear that the usual Sq currents flow at about 120 km in low latitudes, and the equatorial electrojet flows around 105 km apart from them. This structure is in accordance with rocket observation by Davis et al. (1967) (Fig. 12). This separation is also seen at 0000 LT, but the heights are almost the same, though the separation is not clear at 0600 LT. The most

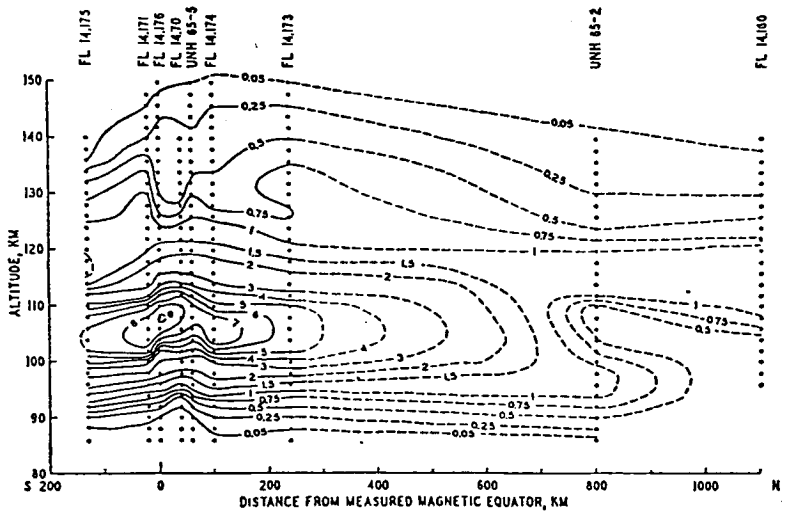

Fig. 12. Cross-sectional profile of the equatorial electrojet obtained from nine rocket flights off the coast of Peru in 1965, normalized to produce ΔH = 100 nT at Huancayo. Circles indicate locations of data points used to obtain the contours of current density in 10^{-6} A/m^2. The right-hand portions of the contours are dashed to indicate uncertainty associated with the relative lack of data for this portion of the diagram. (Figure is from Davis et al. (1967))

remarkable feature appears at 1800 LT. At this time, westward currents exist only near the equator, while currents flow eastward outside of the equatorial region. This reversal can be understood if Fig. 11 is noticed. At lower altitudes, σ_2 is larger than σ_1 (about 10 times at 100 km, see Fig. 1). Therefore the static field (E_t^s) perpendicular to the magnetic field line in the meridional plane plus the induced field (E_t^d) contribute to the eastward current more than that ($E_\phi^s + E_\phi^d$) in the direction of ϕ. As one can see in Fig. 11, at 100 km, j_ϕ driven by $E_\phi^s + E_\phi^d$ ($j_{\phi\phi}$) are only 1/100 ~ 1/1000 of j_ϕ by $E_t^s + E_t^d$($j_{\phi t}$). Therefore if E_t^s ($\simeq E_t^s + E_t^d$) is reversed, j_ϕ is also reversed. Though E_ϕ^s does not change so much in the region from 0° to 20°

in latitude, E_t^s can change sign. At 1800 LT, j_ϕ is reversed only in the equatorial region because of the reversal of E_t^s, and as $E_\phi^s + E_\phi^d$ is much smaller than $E_t^s + E_t^d$ (about 1/200), this reversal extends to more than 200 km in altitude.

3-2. CURRENTS CAUSED BY SEMIDIURNAL TIDAL WINDS

Electrostatic potential distributions at 90 km for (2,2) and (2,4) mode tidal winds are shown in Figs. 13 and 14, respectively. These have the form of four vortices instead of two vortices in the case of diurnal winds. Height integrated currents in the E (90-150 km) (left) and F (150-400 km) (middle) layers and in the total ionosphere (right) are shown in Fig. 15 for (2,2) mode (top) and (2,4) mode (bottom), respectively. Comparing Figs. 13 and 14, we know that the electrostatic fields generated by (2,2) tidal mode mainly exist only in the low latitude region, whereas those by (2,4) mode are distributed worldwide, although the strongest are at about 40° in latitude, which is similar to those by (1,-2) mode (Fig. 5). The difference of these

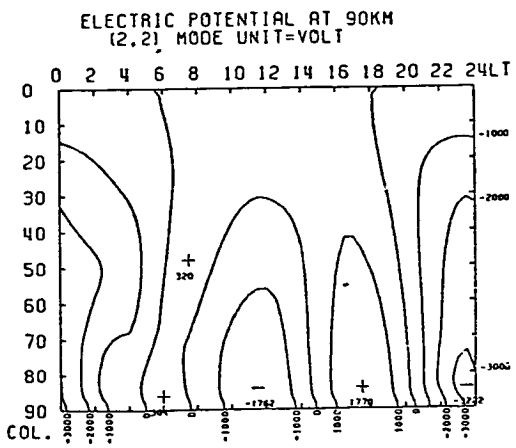

Fig. 13. Electrostatic potential at 90 km generated by (2,2) mode tidal winds. Contours are drawn at every 1000 V.

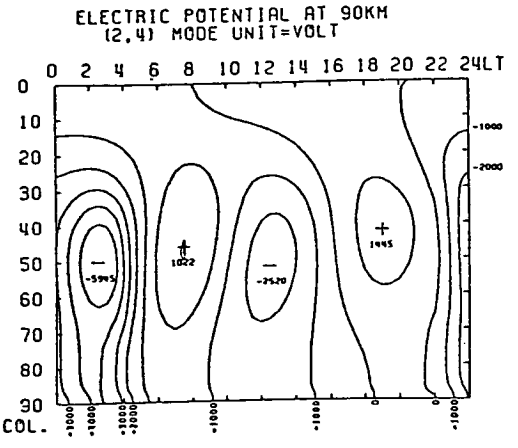

Fig. 14. Same as in Fig. 13 but by (2,4) mode.

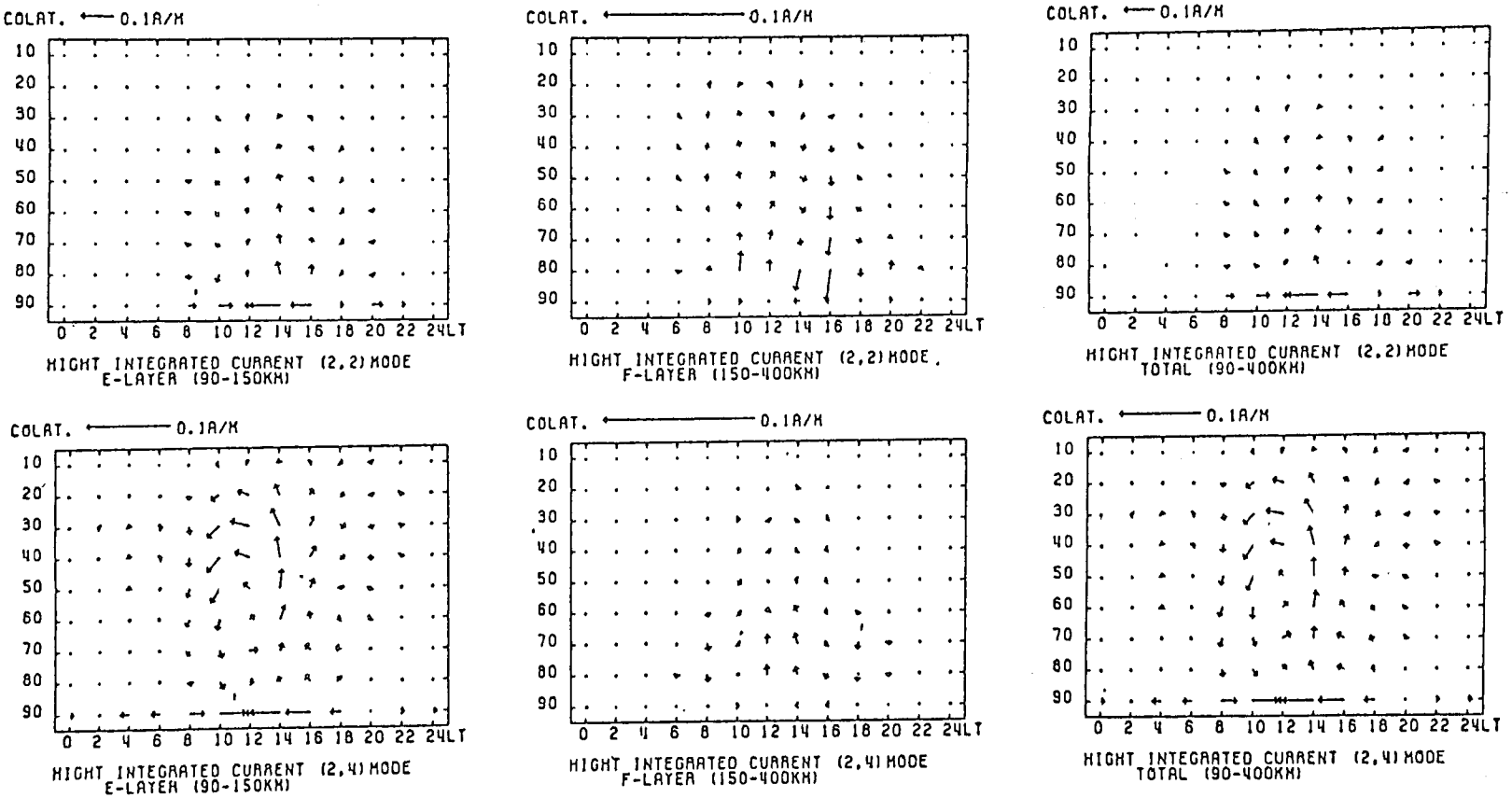

Fig. 15. Height integrated current distribution in the E layer (left), F layer (middle), and total ionosphere (right) for (2,2) mode (top) and (2,4) mode (bottom).

distributions properly reflects the current systems. As shown in Fig. 15, current vortices by the (2,2) mode are situated between 10° and 20° in latitude, while those by the (2,4) mode are between 30° and 40° in latitude. If we remember that the (2,2) mode tidal winds blow principally in low latitude regions, this result is quite natural. To show the detail of height integrated currents in low latitude regions, Fig. 16 gives daily variations of height integrated currents at 10° in latitude (top) and at the equator (bottom) for the (2,2) mode (left) and the (2,4) mode (right). Height integrated currents by the (2,4) mode have an eastward component in the morning and a westward

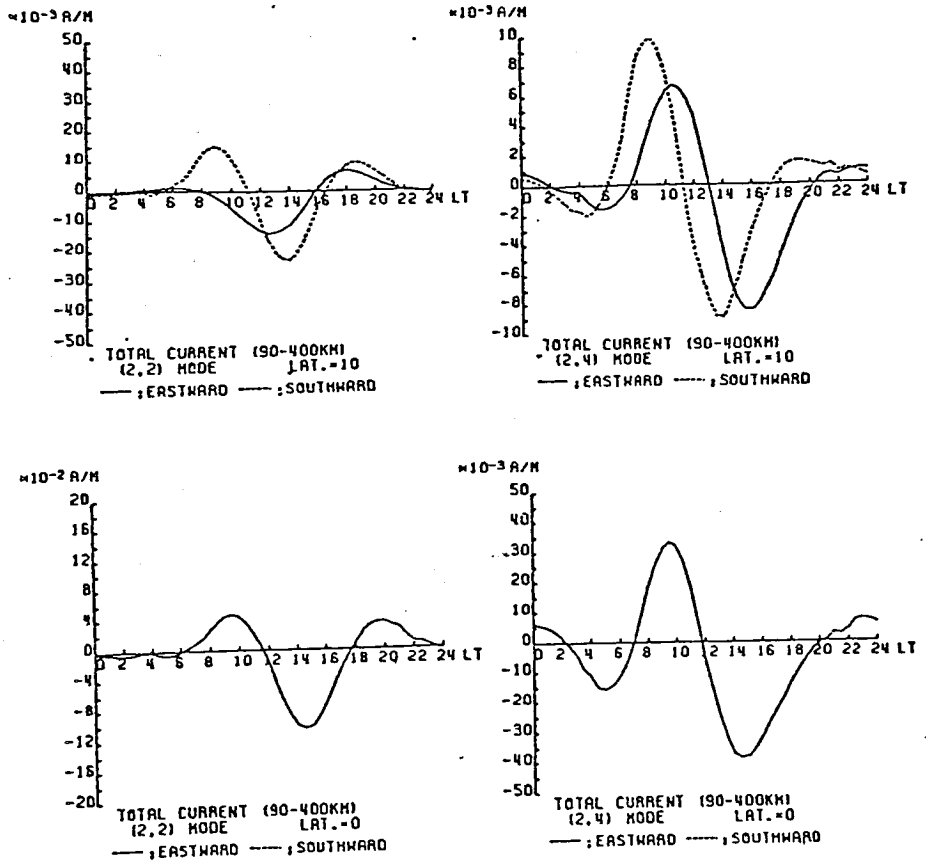

Fig. 16. Daily variation of height integrated currents at 10° in latitude (top) and at equator (bottom) for (2,2) mode (left) and (2,4) mode (right). Solid lines and dotted lines represent eastward and southward currents, respectively. A nick of ordinate represents 5×10^{-3}, 2×10^{-2}, 1×10^{-3}, and 5×10^{-3} A/m for upper left, lower left, upper right and lower right frame, respectively.

one in the afternoon at both places. On the other hand, those by the (2,2) mode have negative peak values at different local time between both places, though at the equator they resemble those by the (2,4) mode. Such locality of currents by the (2,2) mode suggests that this mode is responsible for geomagnetic variations localized in low latitude region, such as the equatorial counter electrojet. This problem is discussed in chapter 6.

Figures 17-20 show eastward current densities (bottom) and currents in the meridional plane (top) for the (2,2) mode (left) and the (2,4) mode (right) in the equatorial region at 1200, 1400, 1600 and 1800 LT, respectively. A meridional vortex current system centered around 120 km in altitude and about 2° in latitude, such as shown for diurnal tidal winds, can be seen in most of these cases, but has a more complex form because the east-west component of currents does not always have the same sign in this region. Change of direction of east-west currents is earlier in higher latitudes and spreads to lower latitudes for the (2,2) mode. This tendency is reversed for the (2,4) mode, and this difference might be useful to distinguish the effects of (2,2) and (2,4) modes.

It is seen that the current intensity calculated here is fairly large. For instance, peak absolute values of height integrated currents at the equator by (2,2) and (2,4) modes are 10.09×10^{-2} A/m and 3.72×10^{-2} A/m, respectively and large compared with that of the (1,-2) mode (5.80×10^{-2} A/m). And current patterns by semidiurnal modes are different from that of a normal

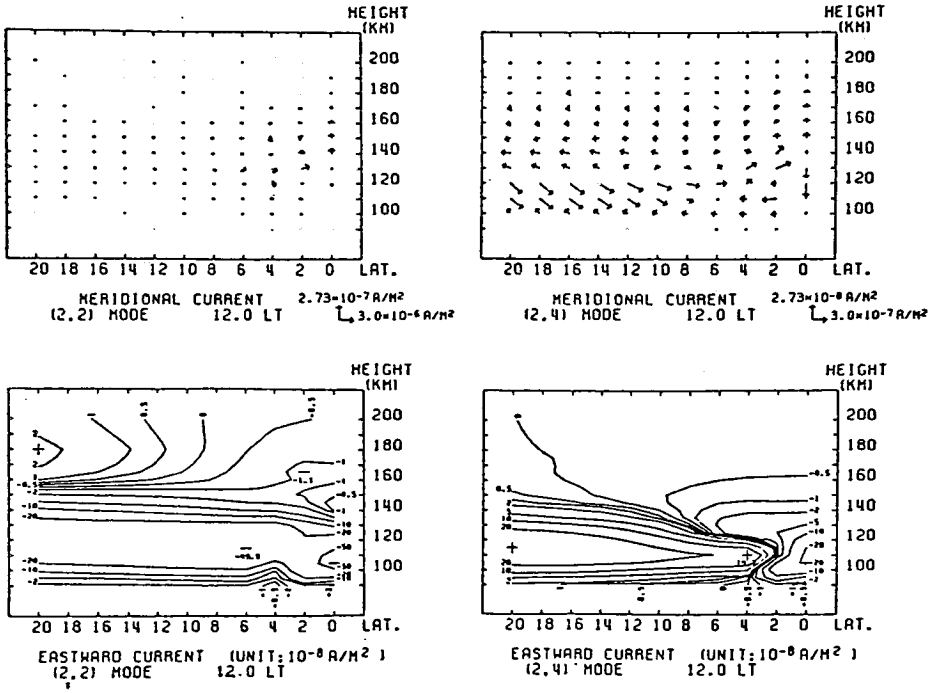

Fig. 17. Meridional current structure (top) and eastward current density distribution (bottom) between 0° and 20° in latitude for (2,2) mode (left) and (2,4) mode (right) at 1200 LT.

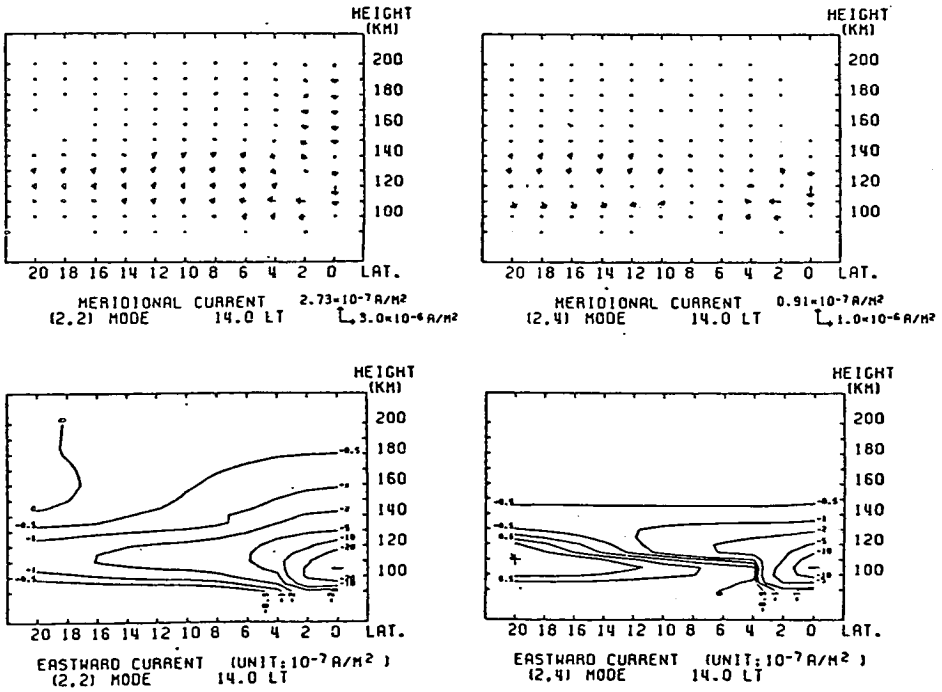

Fig. 18. Same as in Fig. 17 but at 1400 LT.

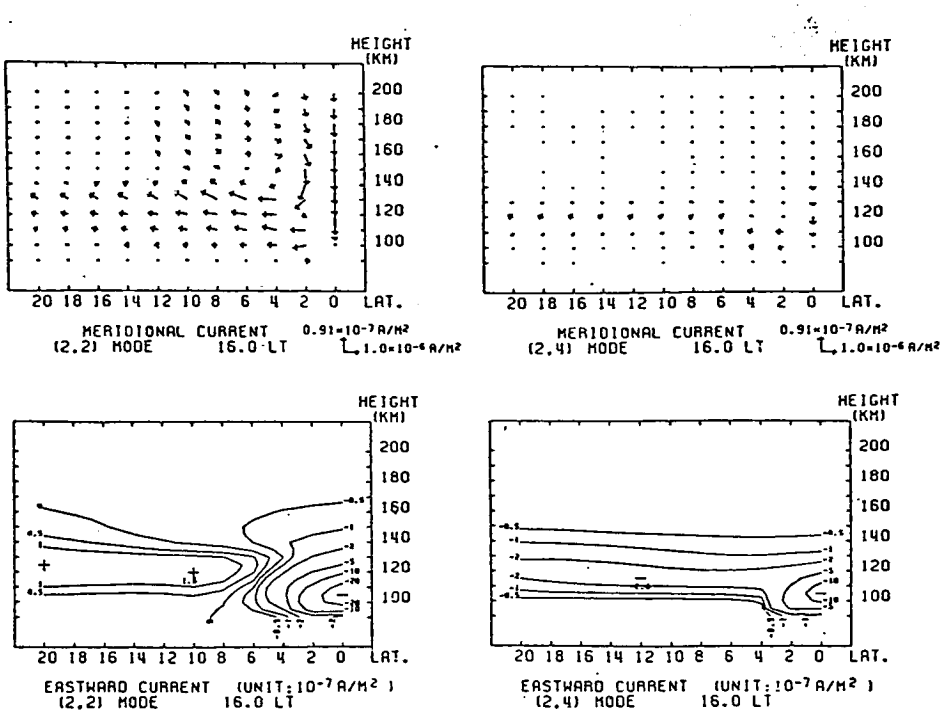

Fig. 19. Same as in Fig. 17 but at 1600 LT.

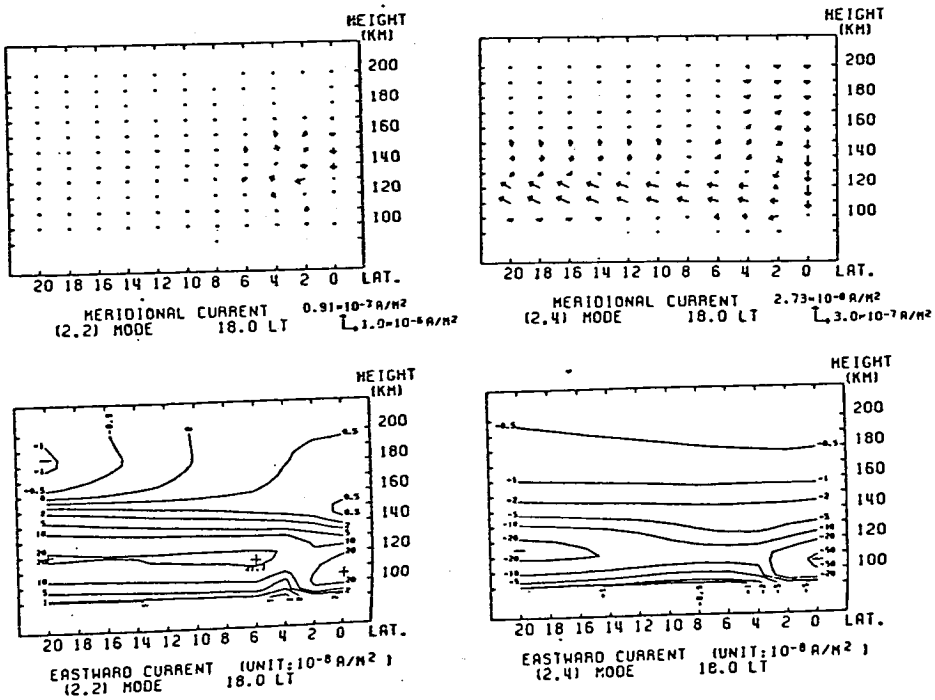

Fig. 20. Same as in Fig. 17 but at 1800 LT.

Sq current system obtained from data analysis (Matsushita and Maeda, 1965). Therefore, if semidiurnal tidal winds are always as strong as in this model compared with diurnal tidal winds, geomagnetic solar quiet daily variation would be different from the observed one. This problem is also discussed in chapter 6.

4.CALCULATION FOR ASYMMETRICAL CASES

In chapter 3, we have calculated three dimensional ionospheric currents under symmetrical condition. However, as strength of the generator in each hemisphere is not equal in general, field-aligned currents flow between two conjugate points and tend to equalize the electrostatic potential at them. A number of workers studied this problem with various simplified assumptions. Van Sabben (1969, 1970) obtained field-aligned currents from the observed magnetic potential. Maeda and Murata (1968) and Maeda (1974) calculated field-aligned currents by asymmetrical dynamo action in the ionosphere using the assumption of two dimensional ionosphere and vertical magnetic field line. Stening (1977a) solved this problem by his equivalent circuit method. Fukushima (1979) examined asymmetrical dynamo in the ionosphere by separating the electrostatic potential into two parts which are produced by Pedersen conductivity only and by the presence of Hall conductivity, respectively. Here, we get three dimensional ionospheric currents and field-aligned currents by asymmetrical ionospheric dynamo self-consistently, by applying the method presented in chapter 2.

When we consider asymmetrical cases, equation (11) cannot be solved considering one hemisphere only, but need to take two hemispheres into consideration simultaneously, because field-aligned currents flow between two conjugate points. Therefore we integrate equation (7) along the magnetic field line in the region of the ionosphere of both northern and southern hemispheres. Under the assumption of infinite parallel conductivity as in chapter 2, the reselt has the form

$$A\frac{\partial^2 S}{\partial t^2} + B\frac{\partial^2 S}{\partial \phi^2} + D\frac{\partial S}{\partial t} + E\frac{\partial S}{\partial \phi} + F$$

$$= [\, - h_\phi h_t j_s]_{s_1}^{s_2} + [\, - h_\phi h_t j_s]_{s_3}^{s_4} \qquad (12)$$

where

$$A = \int_{s_1}^{s_2} a\, ds + \int_{s_3}^{s_4} a\, ds \quad \text{etc.}$$

and s_1, s_2, s_4 and s_3 are values of s at lower and upper boundary in the northern and southern hemispheres, respectively. Considering Pedersen (σ_1) and Hall (σ_2) conductivities are almost zero outside of the ionosphere, we assume that currents which flow upward from the ionosphere do not leak transversely, but entirely flow into the ionosphere of the opposite hemisphere at the conjugate point (i.e. j_s is equal at $s=s_2$ and $s=s_3$). At the lower boundaries, we assume that vertical current is zero, which is the same as in chapter 3. Then equation (12) becomes

$$A\frac{\partial^2 S}{\partial t^2} + B\frac{\partial^2 S}{\partial \phi^2} + D'\frac{\partial S}{\partial t} + E'\frac{\partial S}{\partial \phi} + F' = 0 \qquad (13)$$

where

$$D' = D + (\sigma_1 h_\phi \cot I)_{s=s_1} + (\sigma_1 h_\phi \cot I)_{s=s_4}$$

$$E' = E + (\sigma_2 h_t \cot I)_{s=s_1} + (\sigma_2 h_t \cot I)_{s=s_4}$$

$$F' = F + ((\sigma_1 vB + \sigma_2 uB_r)\cot I)_{s=s_1} + ((\sigma_1 vB + \sigma_2 uB_r)\cot I)_{s=s_4}$$

Solving equation (13) by a relaxation method using a boundary condition $j_r = j_t = 0$ at the lower boundary of the equatorial ionosphere, we get the electrostatic potential, and then three dimensional ionospheric currents by equations (4) and (6) and by integration of equation (7). Field-aligned currents generated by the dynamo action in the ionosphere are obtained as j_s at $s=s_2$ or $s=s_3$.

In the following calculations, we used a three dimensional conductivity model fundamentally same as in the calculation for symmetrical cases in chapter 3, and wind model of (1,-2) mode presented by Salah and Evans (1977) (Fig. 4), extending it up to 400 km on the assumption that the wind above 200 km has the same amplitude and phase as those at 200 km.

4-1. CALCULATION FOR THE UT VARIATION OF SQ CURRENTS

Difference between geographic and geomagnetic coordinates causes UT variation of Sq currents. Conductivity and tidal winds of (1,-2) mode are assumed to be distributed in conformity with the geographic coordinate system. Geomagnetic field is considered as a dipole field. We transfer conductivity and winds to the geomagnetic coordinate system and calculate the ionospheric currents and attendant field-aligned currents at the times of 00 and 06 UT. In the cases of 12 and 18 UT, they are the north-south reversal of those at 00 and 06 UT, respectively.

Figures 21, 22 and 23 show the electrostatic potential distribution, height integrated currents and field-aligned currents at 00 UT and 06 UT. Figures 24 and 25 represent currents in the noon meridional plane (top) and eastward currents (bottom) at 00 and 06 UT, respectively. From Figs. 21 and 22 it is seen that though electrostatic potential distribution is not so different, horizontal current system shifts southward (northward) as a whole in geomagnetic coordinate system at 06 UT (18 UT) except for the equatorial electrojet. Vortex center of the currents in the northern

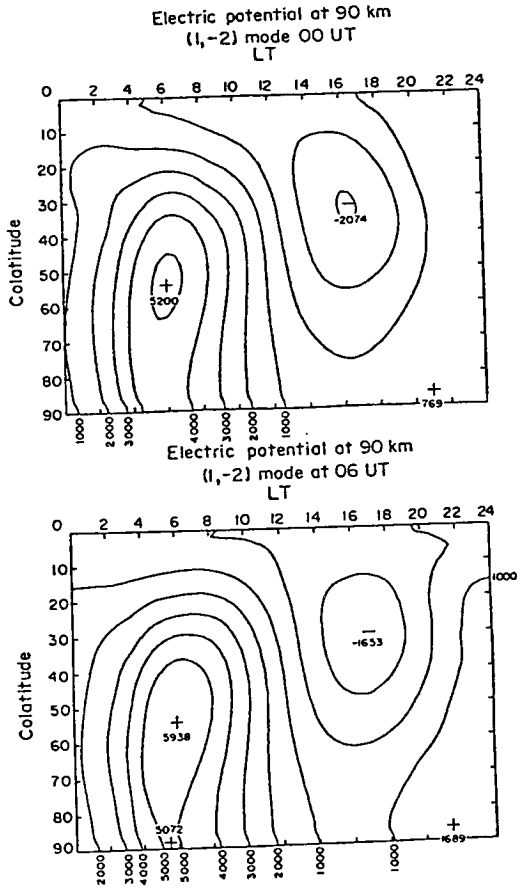

Fig. 21. Electrostatic potential at 90 km at 00 UT (top) and at 06 UT (bottom). Ordinates represent geomagnetic colatitude and abscissas magnetic local time.

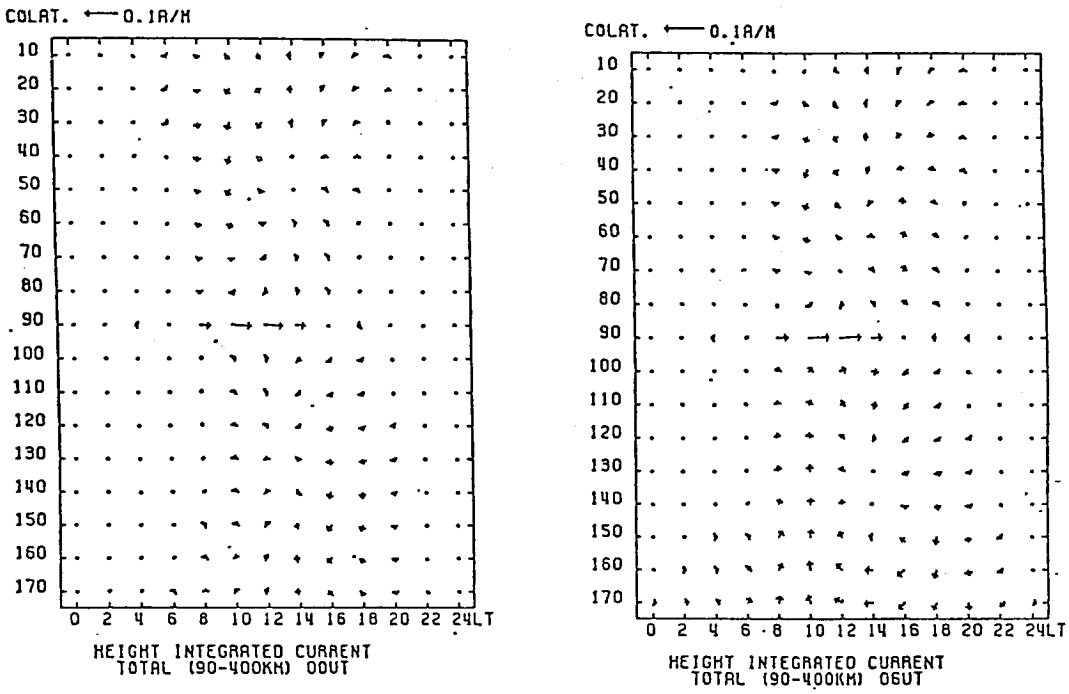

Fig. 22. Ionospheric height integrated currents at 00 UT (left) and at 06 UT (right). Ordinates and abscissas are the same as in Fig. 21.

hemisphere situates at about 50°, 62°, 52° and 44° in geomagnetic colatitude and total currents flowing between the vortex center and the geomagnetic equator are 4.5×10^4, 2.6×10^4, 4.5×10^4 and 5.6×10^4 A at 00, 06, 12 and 18 UT, respectively. These changes are caused by the movement of conductivity and wind distribution relative to the geomagnetic coordinate system, and variation of the current intensity is consistent with the result of data analysis (Suzuki, 1979), though movement of current vortex center is not well reproduced.

Field-aligned currents flow by north-south asymmetry of ionospheric dynamo action. Figure 23 shows that intensity of these currents by the discordance of geographic and geomagnetic axes does not change by UT so much, but has

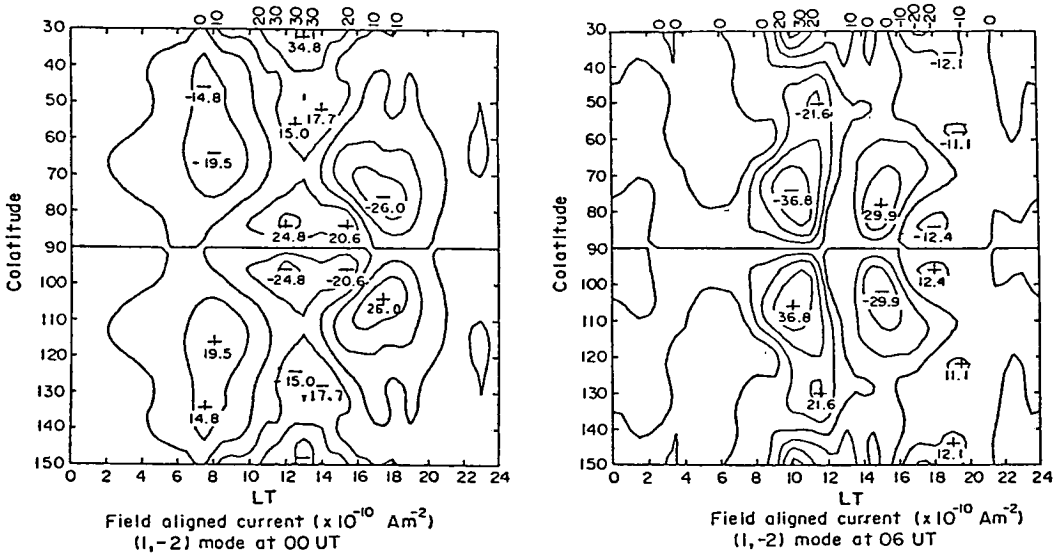

Fig. 23. Distribution of field aligned currents (j_S) at 00 UT (left) and 06 UT (right). Positive values correspond to downward currents into the ionosphere. Ordinates and abscissas are the same as in Fig. 21.

peak values of about $2 \sim 4 \times 10^{-9}$ A/m^2. Total field-aligned currents are about 5×10^4 A at both UT's, which is about as much as currents in the ionosphere.

Figure 24 and 25 show that the equatorial electrojet and the meridional current system incidental to it keep symmetry about the geomagnetic equator, though low latitude eastward currents outside of the equatorial region are affected by the UT variation. This is quite reasonable because the eqatorial electrojet is dominated mainly by the configuration of the geomagnetic field.

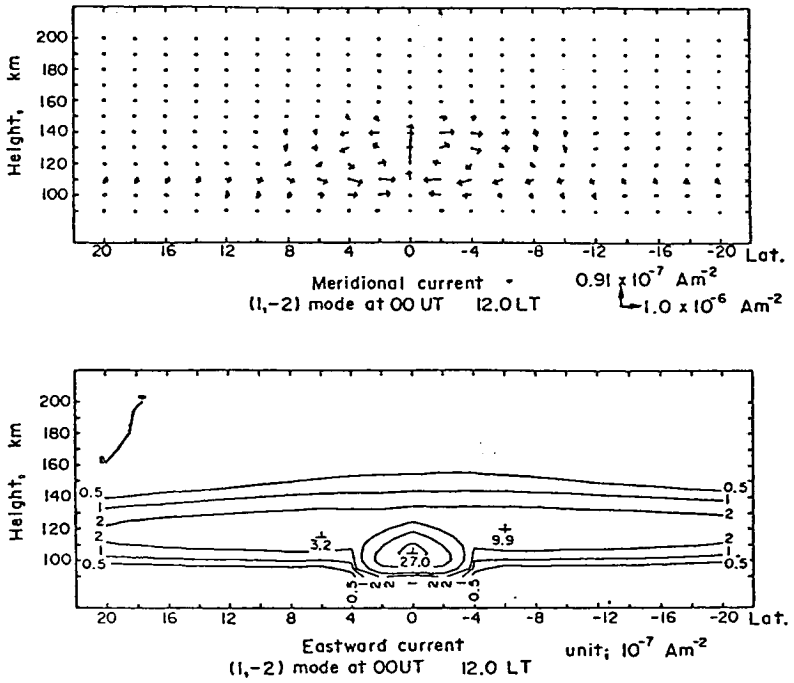

Fig. 24. Meridional current system (top) and eastward current density distribution (bottom) near the equator at 1200 MLT and at 00 UT.

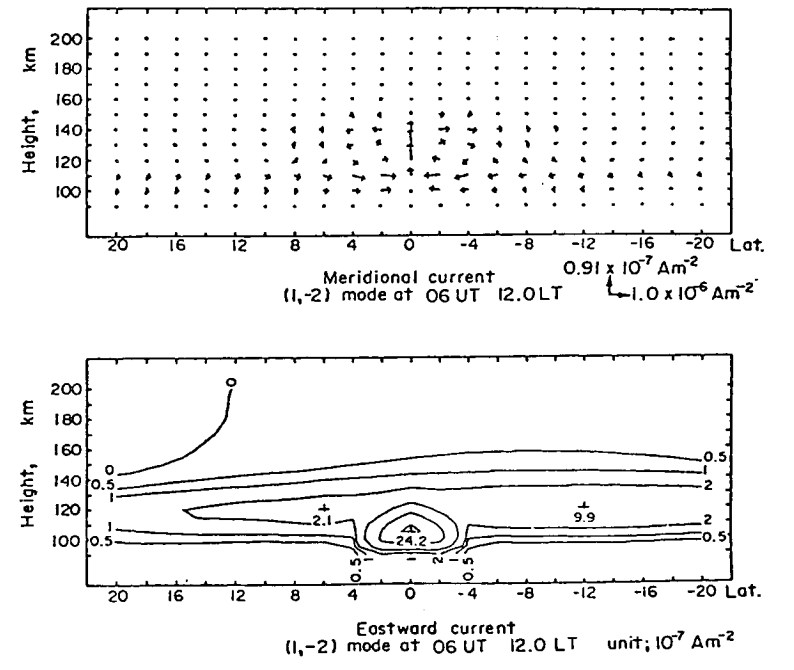

Fig. 25. Same as in Fig. 24 but at 06 UT.

4-2. CALCULATION FOR SOLSTICE CONDITION

Asymmetry of ionospheric dynamo is also caused by conductivity asymmetry. At solstice it is expected that the asymmtry in conductivity distribution is caused by the inequality of solar radiation between both hemispheres. Here we assume that conductivity distribution and tidal winds of (1,-2) mode are shifted by 23.5° in latitude from the equinox condition. Discrepancy between the geographic and geomagnetic coordinate systems is ignored in this time. There may be a difference in amplitude and phase distribution of (1,-2) mode tidal winds, and asymmetrical tidal winds be more improtant, but these are also ignored.

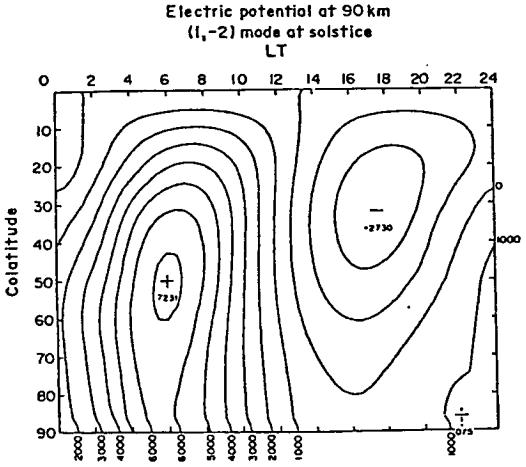

Fig. 26. Electrostatic potential at 90 km at solstice.

Calculated potential distribution, height integrated currents, field-aligned currents and three dimensional currents near the equator at noon are shown in Figs. 26, 27, 28 and 29, respectively. In these figures, the northern hemisphere corresponds to the winter one. Figure 27 shows that the westward currents in the winter (northern) hemisphere decreases,

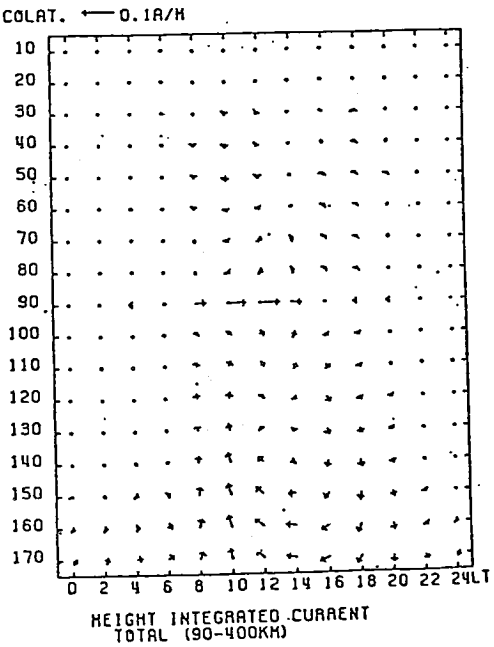

Fig. 27. Ionospheric height integrated currents at solstice.

whereas those in the summer (southern) hemisphere increase. Eastward currents are not so different in both hemispheres, and so negative (positive) charge accumulation is expected in the morning (afternoon) region of the winter hemisphere, if there are no field-aligned currents which carry charges between both hemispheres. This is caused by the larger conductivity difference in both hemispheres in higher latitude zone. Calculated field-aligned current distribution presented in Fig. 28 is

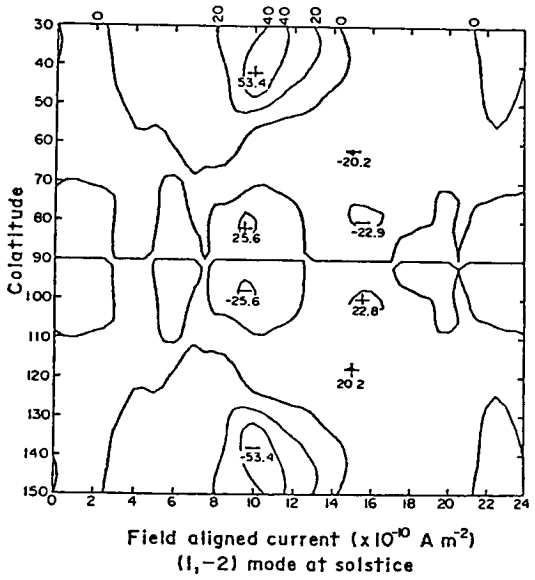

Fig. 28. Distribution of field-aligned currents into the ionosphere at solstice.

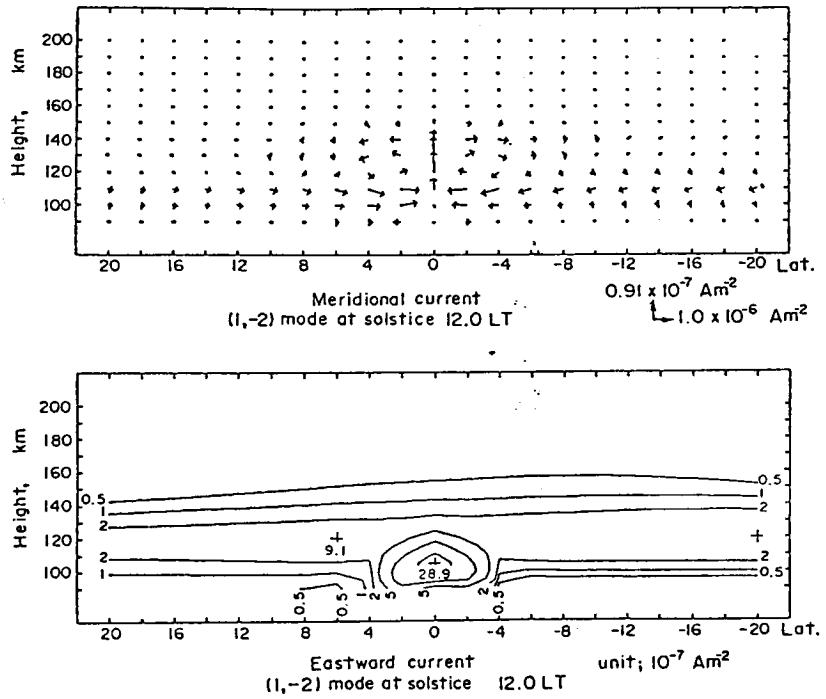

Fig. 29. Meridional current system (top) and eastward current density distribution (bottom) near the equator at solstice.

almost like that expected from the above consideration. That is, the currents flow mainly from the summer to the winter hemisphere in the morning and vice versa in the afternoon, and this is consistent with the result by Van Sabben (1970) and with observation by satellite (Maeda et al., 1982). The density of those currents is about $2 \sim 5 \times 10^{-9}$ A/m^2 and the intensity is 7×10^4 A, which is a little larger than the currents in the ionosphere between the current vortex and and the equator ($\sim 5 \times 10^4$ A). Figure 29 shows that currents in the equatorial region scarcely become asymmetric, though currents outside of the region are stronger in the summer than in the winter hemisphere. This symmetry of the equatorial electrojet is the same as in chapter 4-1.

5. CALCUTION OF IONOSPHERIC CURRENTS OF MAGNETOSPHERIC ORIGIN

Field-aligned currents of magnetospheric origin which was first found by Zmuda et al. (1966, 1967) exist even in quiet periods (Iijima and Potemra, 1976) and are believed to play an important role in geomagnetic daily variations in the polar region such as Sq^P and to have some influence on the Sq current system in middle and low latitudes. Matsushita (1971) has presented a hypothesis that the primary source of quiet day ionospheric electric currents may not be dynamo action in the ionosphere. Though this hypothesis is not supported by Richmond et al. (1976), some of the variation of the Sq current system may be attributed to origins outside of the ionosphere (e.g. Butcher and Brown, 1980, 1981a, b; Butcher, 1982). Calculations of global ionospheric currents assuming a two-dimensional ionosphere (thin shell model) have been made by

many workers by applying external electric fields (Iwasaki and Nishida, 1967; Maeda and Maekawa, 1973; Maltsev et al., 1973) or field-aligned currents (Yasuhara et al., 1975; Yasuhara and Akasofu, 1977; Maekawa and Maeda, 1978; Barbosa, 1979; Kamide and Matsushita, 1979a, b; Maekawa, 1980). Here, using the method presented in chapter 2, we calculate three dimensional ionospheric currents in the ionosphere generated by field-aligned currents of magnetospheric origin.

Putting wind velocities (u,v) zero and $j_S = j_f$ at $s=s_2$ in equation (11), we get the equation determining a electrostatic potential distribution in the ionosphere as follows:

$$A\frac{\partial^2 S}{\partial t^2} + B\frac{\partial^2 S}{\partial \phi^2} + D'\frac{\partial S}{\partial t} + E'\frac{\partial S}{\partial \phi} = -h_t h_\phi j_f \qquad (14)$$

where j_f is determined from the distribution of field-aligned currents. Iijima and Potemra (1978) show that there are also some field-aligned currents even during quiet periods, and that the net currents (region 1 plus region 2) exist almost only in the dayside region. Field-aligned currents are obtained also from magnetic records along a meridional chain (Akasofu et al., 1980; Kamide et al., 1981). Akasofu et al. (1980) showed from data for the equinox that on quiet days the field-aligned currents and the ionospheric currents are mostly confined to the dayside half of the polar region. This is quite natural because the conductivity in the daytime is much greater than at night without conductivity enhancement in the auroral region. Considering these

observational results, we have made a model of field-aligned current distribution as follows:

$$j_f = j_0 \sin(2(\phi_0 - \phi))\left(\frac{1 + \cos(36(\theta - \theta_0))}{2}\right)$$

in the dayside half belt of colatitude $10° \leq \theta \leq 20°$, and zero elsewhere, where $\theta_0 = 15°, \phi_0 = 180°$ and ϕ is measured from midnight. $j_0 = 1 \times 10^{-7}$ A/m^2 and positive j_f means currents into the ionosphere (see Fig. 30). Total currents flowing from or into the ionosphere are 2×10^5 A, which is not so inadequate compared with observations by TRIAD (Iijima and Potemra, 1978) or with that deduced from magnetic records taken along a meridional chain (Akasofu et al., 1980) and with simulations by Kamide and Matsushita (1979a) for quiet conditions. No auroral enhancement of conductivity is taken into consideration and symmetry with respect to the equator is assumed. Therefore we have to limit our consideration to quiet conditions during the equinox.

Figure 31 shows the electrostatic potential distribution.

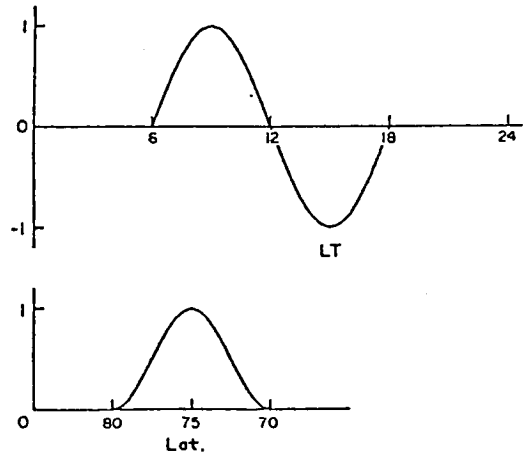

Fig. 30. Model of input field-aligned currents. Daily and latitudinal distributions are shown in top and bottom panels, respectively.

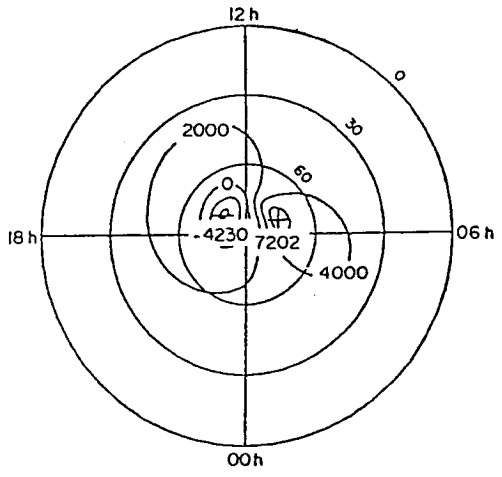

Fig. 31. Electrostatic potential at 90 km. Contours are drawn at every 2000 V. The largest circle represents the equator.

As field-aligned currents are assumed to exist only in the dayside, electrostatic fields are distributed mainly in the dayside and relatively weak because of high conductivity, and comparable to those of the ionospheric wind dynamo (∿ 10,000 V). This result may be changed by introducing net field-aligned currents in the nighttime region. Figure 32 gives the height integrated currents in the E-layer (90-150 km) (a), F-layer (150-400 km) (b) and total ionosphere (c), respectively. The total currents obtained here are similar to those deduced by Kamide and Matsushita (1979a) for quiet conditions, at least in the dayside region. E-layer currents mainly contribute to the total currents and have similar features to them. On the contrary, F-layer

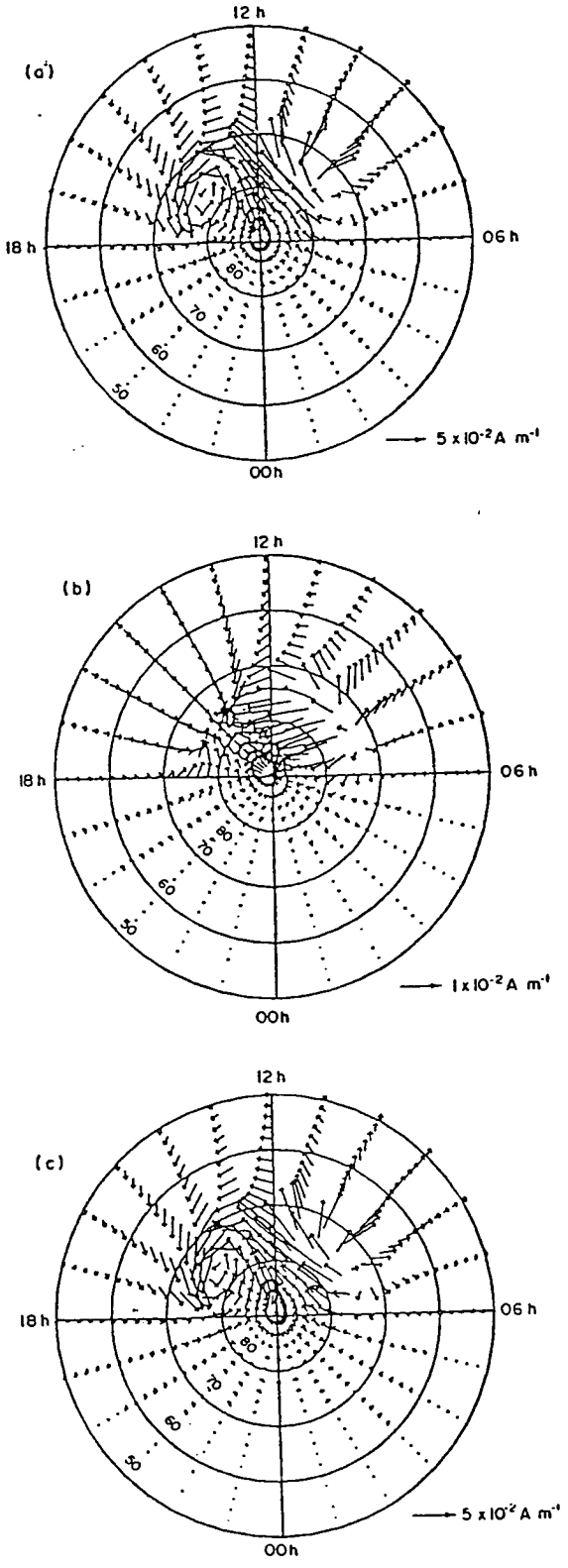

Fig. 32. Height integrated current distribution in the (a) E-layer (90-150 km), (b) F-layer (150-400 km) and (c) total ionosphere (90-400 km) by field-aligned currents of magnetospheric origin. The largest circles represent 50° in latitude.

currents diverge in the morning and converge in the afternoon. This is natural considering that the Pedersen conductivity (σ_1) is dominant over the Hall conductivity (σ_2) at higher altitudes.

Figure 33 (a)-(d) shows the daily variation of ionospheric currents at latitudes of 0°, 20°, 40° and 60°, respectively. Figure 34 represents the latitudinal distribution of height integrated ionospheric currents at 1000 LT when eastward currents are a maximum at the equator. It is easily seen from Figs. 33 and 34 that the currents in the longitudinal direction flow almost eastward and practically exist only in the daytime. At the equator these currents have a peak value of 1.5×10^{-2} A/m at 1000 LT, which is much weaker

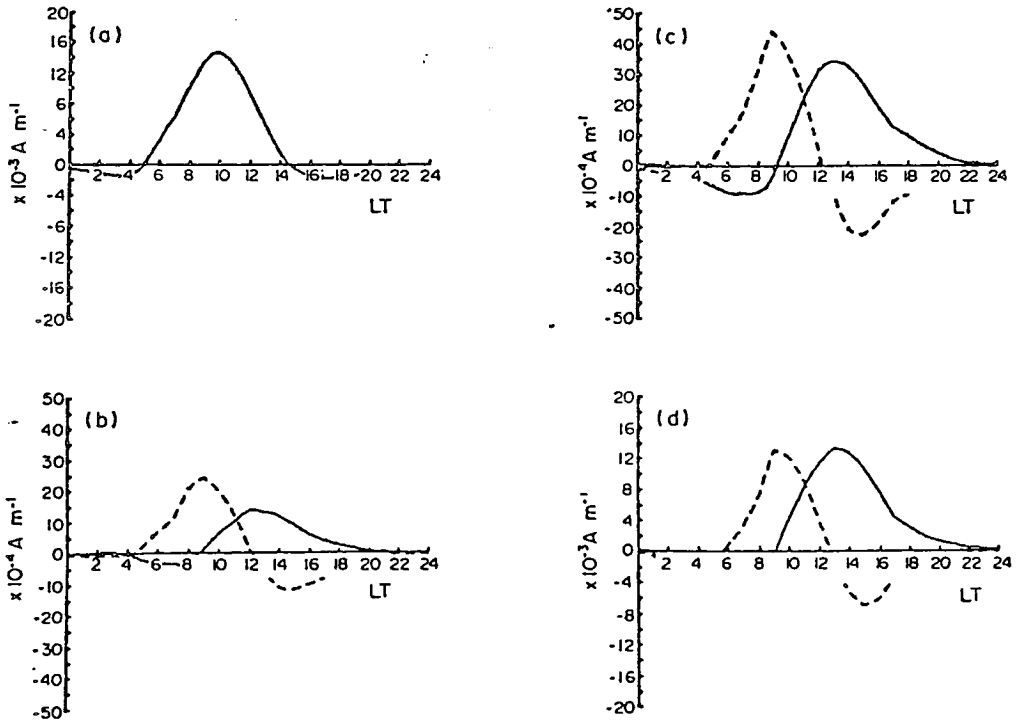

Fig. 33. Daily variation of height integrated currents at latitudes of (a) 0°, (b) 20°, (c) 40° and (d) 60°, respectively. Solid and dotted lines represent eastward and southward (equatorward) currents, respectively.

than the usual equatorial electrojet current (∿0.1 A/m). In the region of lower latitudes, ionospheric currents by field-aligned currents are also much weaker than those of ionospheric dynamo and have a similar daily variation pattern to Sq currents. On the other hand, they are opposite in direction to Sq currents in the region of latitudes higher than the vortex of the Sq currents. Therefore the hypothesis by Matsushita (1971) that the primary source of quiet day ionospheric currents is not ionospheric dynamo but magnetospheric convection, is not supported by our calculation. This result agrees with that of Richmond et al. (1976).

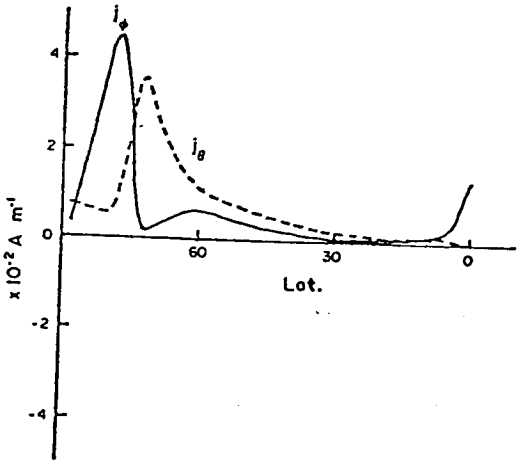

Fig. 34. Latitudinal distribution of height integrated currents at 1000 LT. Lines are same as in Fig. 33.

The three dimensional ionospheric current distribution at 1000 LT is given in Fig. 35. This figure shows that westward currents exist at lower altitudes between 20° and 74° in latitude. These westward currents are cancelled by eastward currents at higher altitudes and do not appear in the total height integrated current (Fig. 34). This structure comes from the height distribution of σ_1 and σ_2. That is, electric fields have small southward (E_s) and large eastward (E_e) components there (Fig. 31), and they make westward ($\sigma_2 E_s$) and eastward ($\sigma_1 E_e$) currents, respectively, and hence although the electrostatic fields do not vary with altitude, currents flow westward in the

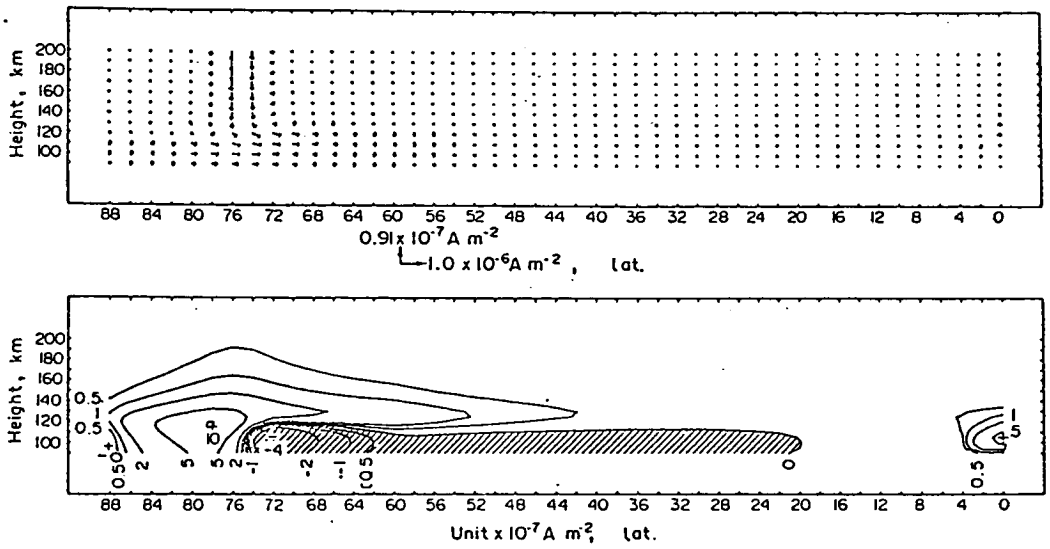

Fig. 35. Meridional current structure (top) and eastward current density distribution (bottom) at 1000 LT.

lower region where σ_2 is dominant, and eastward in the higher region where σ_1 is dominant, respectively. In the equatorial region the equatorial electrojet and the meridional current system incidental to it are also seen.

This calculation is made by using simplified field-aligned current model. A more detailed distribution of input field-aligned currents including double-layer strucure and cusp region field-aligned currents, and also a weak conductivity enhancement which may exist even on quiet days, will be necessary to discuss the effects of field-aligned currents of magnetospheric origin on ionospheric currents more precisely. If the exact distribution of field-aligned currents and three dimensional distribution of conductivity in the ionosphere are known, three dimensional currents at any point in the ionosphere can be calculated by our method. Such observations, especially the three dimensional distribution of conductivity are desirable.

6. AN ASSESSMENT OF VARIOUS SOURCES AS GENERATOR OF SQ AND ITS DAY-TO-DAY VARIATION

As Maeda (1955, 1957) and Kato (1956) showed from geomagnetic Sq variation, ionospheric wind necessary to produce Sq currents is diurnal. By simulation Stening (1969) and Tarpley (1970b) obtained the result that diurnal tidal winds, especially of (1,-2) mode, mainly contribute to Sq currents, and Richmond et al. (1976) also supported this idea. In our calculations, tidal winds of (1,-2) mode are shown to produce ionospheric currents similar to those obtained from data analysis. By our result, however, effects of semidiurnal tidal winds are rather large, and if used wind model (Salah and Evans, 1977) is quite adequate, observed ionospheric currents are not well reproduced. This suggests that the wind model may not be correct to express the globally typical wind pattern. For example, Rees et al. (1979) reports that the semidiurnal winds are weak or absent on June 29 and 30, 1974 by rocket observation, and recently Mazaudier (1982) and Mazaudier and Blanc (1982) find by incoherent scatter radar observation at St. Santin that diurnal winds and semidiurnal tidal winds are larger and smaller than those by Salah and Evans (1977), respectively. Volland and Grellmann (1978) calculated a hydromagnetic dynamo of the atmosphere using a uniform conductivity model and concluded that propagating semidiunal tidal winds attenuate strongly at higher altitudes. On the other hand, Rishbeth (1971a) first pointed out that daily pressure variation due to solar heating generates currents in the F-region, and Rishbeth (1971b), Heelis et al. (1974) and Matuura (1974) evaluated the effects of F-region dynamo on the electric fields and confirmed

that F-region winds, which seem to be mainly diurnal, modify the fields. This idea is supported by observations of electric fields at Jicamarca (magnetic dip 2° N) (Woodman, 1970; Woodman et al., 1977; Fejer et al., 1979). In fact it is doubtful that observed winds at middle latitude (e.g. Millstone Hill which is used by Salah and Evans is 57° N in geomagnetic latitude) can extend to equatorial region according to classical tidal theory, especially at higher altitudes where effects of ion drag become important. For example, Richmond et al. (1976) showed that tidal winds of (1,-2) mode are modified to (1,-2)* mode by ion drag. As a result, for instance, westward winds at low latitudes around 1800 LT change to eastward, and eastward electric currents extend further into evening. In fact winds at 1800 LT at low latitudes obtained from geomagnetic Sq are eastward (Maeda, 1955). Furthermore Maeda et al. (1982) recently find meridional currents in the F-region of low latitude duskside, and Takeda and Maeda (1983) show that eastward winds are necessary to explain this phenomenon. Observation of neutral wind in low latitude around sunset (King-Hele and Walker, 1977) surely shows the existence of eastward winds above 170 km in altitude. Therefore it is probable that non propagating diurnal tidal winds such as (1,-2)* according to Richmond et al. (1976) blow eastward at low latitudes in the evening because of the effects of ion drag and this is responsible for maintenance of eastward equatorial electrojet.

Semidiurnal tidal winds propagating from lower altitudes such as (2,2) or (2,4) mode may be affected by the situation of mesosphere and lower thermosphere and therefore possible to change and to cause day-to-day variation of Sq currents. One of the most remarkable phenomena of the day-to-day

variation is the equatorial counter electrojet. This is a phenomenon that the equatorial electrojet sometimes reverses from eatsward to westward especially in the afternoon. This is supposed to be a part of the global current system (Takeda and Maeda, 1980). Locality of currents by tidal winds of (2,2) mode shown in chapter 3 suggests that the equatorial counter electrojet may be caused by the enhamcement of this mode. Of cource, the counter electrojet may be partly attributed to the other effects such as lunar tide (Rastogi, 1973; Mayaud, 1977) and gravity waves (Raghavarao and Anandarao, 1980). It is, however, generally believed that the lunar effect is modulation and not the main source of the counter electrojet. Recently, Bhargava et al. (1980) studied the afternoon counter electrojet in India and showed that lunar control is only 25 % at maximum and gravity waves cannot totally explain this phenomenon. On the other hand, Stening (1977b) examined magnetic variations of worldwide stations at occasions of the equatorial counter electrojet in the afternoon and found that in some cases they are explained by semidiurnal winds of (2,2) mode. Bhargava and Sastri (1977) compared days with afternoon counter electrojet, with those without it in the Indian region statistically and found that at the equatorial stations (Trivandrum, Kodaikanal, and Annamalainagar) counter electrojet is accompanied with increase of H component from normal daily variation value in the morning, and that similar additional variation is also seen at Alibag (9.4° N in geomagnetic latitide) with a little phase lag, though its amplitude is rather small (Fig. 36). These features may not be interpreted by (2,2) mode only

but by the mixture of (2,2) and (2,4) modes (see Fig. 16). From above discussions it may be inferred that on normal days effects of diurnal tidal winds are dominant in higher altitudes and make the normal Sq current system and that on some days semidiurnal tidal winds propagating from below become strong possibly by change of propagation condition, and cause day-to-day variation of Sq currents such as the equatorial counter electrojet.

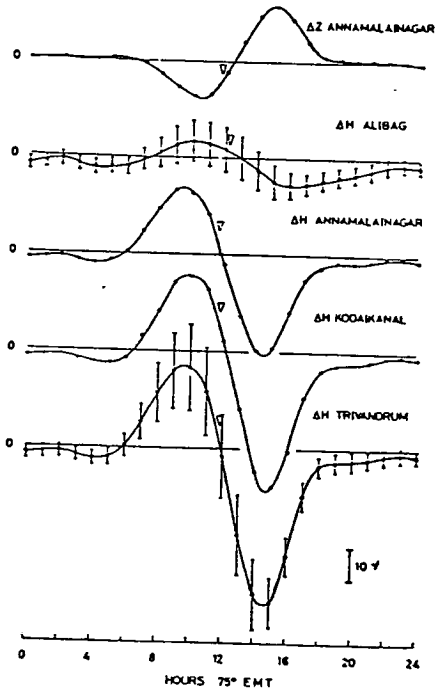

Fig. 36. Diurnal variation of the additional field, on days with the occurrence of counter electrojet afternoon events in the horizontal intensity of the earth's magnetic field, ΔH, at Trivandrum, Kodaikanal, Annamalainagar and Alibag, and also in vertical intensity, ΔZ, at Annamalainagar. (Figure is from Bhargava and Sastri (1977))

To examine the effects of field-aligned currents of magnetospheric origin on Sq current system, Fig. 37 gives the total height integrated currents at 60° (top) and 20° (bottom) in latitude which are the sum of those by (1,-2) mode tidal winds (chapter 3) and those by field-aligned currents of magnetospheric origin (chapter 5) multiplied by a factor of zero (first column), 0.5 (second column), 1 (third column), 2 (fourth column), respectively. From this figure, it is clear that the effects of field-aligned currents of magnetospheric origin are not so important and do not change the

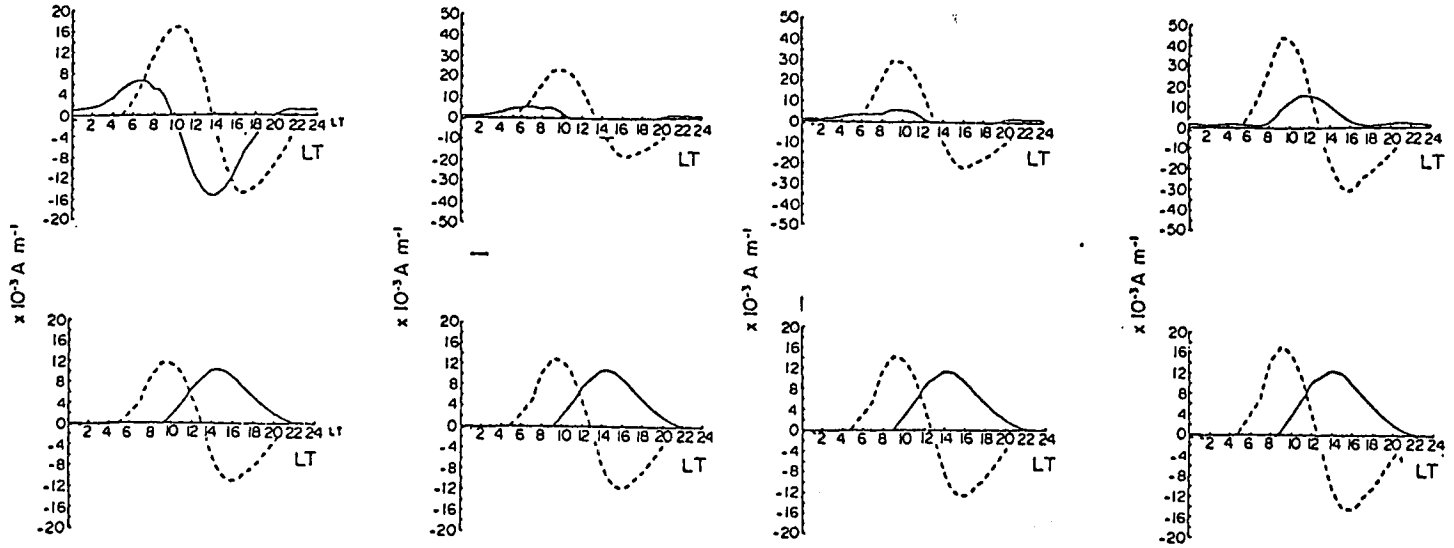

Fig. 37. Daily variation of height integrated currents at a latitude of 60° (top) and 20° (bottom), respectively, adding calculated currents by field-aligned currents of magnetospheric origin multiplied by a factor of 0 (first column), 0.5 (second column), 1 (third column), and 2 (fourth column) to currents by (1,-2) mode tidal winds. Solid and dotted lines represent eastward and southward (equatorward) currents, respectively.

daily variation pattern of currents so much in the lower latitude region, at least in the case of quiet periods in which field-aligned currents are represented by our model. Therefore, day-to-day variations of the Sq currents in low latitudes during quiet periods do not seem to be mainly caused by field-aligned currents of magnetospheric origin but by other effects such as semidiurnal tidal winds propagating from below. On the contrary, in the higher latitude region, ionospheric currents by field-aligned currents alter the Sq current pattern significantly and may reverse the direction of westward currents to eastward in the daytime. Abnormal Sq currents discussed by Butcher and Brown (1980) may be interpreted by such an effect, and understood as the results of the variations of field-aligned currents controlled by interplanetary medium parameters shown by Feldstein et al. (1982). If we use more precise models of field-aligned currents and conductivity, this could be explained more clearly.

7. CONCLUSIONS

Ionospheric currents caused by tidal winds or field-aligned currents of magnetospheric origin are calculated three dimensionally by using magnetic field line coordinate system with the assumption of infinite parallel conductivity. Using the results of the calculations, their contribution to Sq currents and variation of Sq are examined. The followings are revealed.

1. Meridional current system in the equatorial region exists in most cases, only changing its shape and direction according to the electric fields

and winds.

2. Height integrated currents by tidal winds of (1,-2) mode can explain the observed Sq variation best. Those by semidiurnal modes are suspected to cause day-to-day variation of Sq in low latitudes, such as the equatorial counter electrojet. Field-aligned currents of magnetospheric origin have much effect on Sq in higher latitudes, but do not seem to be the main cause of day-to-day variation at lower latitudes during quiet periods.
3. UT variation of Sq currents is partly explained by the effects of discordance between geographic and geomagnetic coordinates. Field-aligned currents generated by asymmetrical dynamo at the solstice are in accordance between our calculation and observations.

Acknowledgments

This research was performed under the guidance of Prof. H. Maeda at our institute. The numerical computations were made by using facilities at the Data Processing Center of Kyoto University.

REFERENCES

Akasofu, S.-I., J. Kisabeth, B.-H. Ahn, and G. J. Romick, The Sq magnetic variation, equivalent current, and field-aligned current distribution obtained from the IMS Alaska meridian chain of magnetometers, J. Geophys. Res., 85, 2085-2091, 1980.

Baker, W. G., Electric currents in the ionosphere, II, The atmospheric dynamo, Philos. Trans. R. Soc. London, A246, 281-294, 1953.

Barbosa, D. D., Field-aligned current sources in the high-latitude ionosphere, Ann. Geophys., 35, 111-119, 1979.

Bartels, J., and H. F. Johnston, Geomagnetic tides in horizontal intensity at Huancayo, Terr. Mag. Atmos. Electr., 45, 269-308, 1940.

Bhargave, B. N. and N. S. Sastri, A comparison of days with and without occurrence of counter-electrojet afternoon events in the Indian region, Ann. Geophys., 33, 329-332, 1977.

Bhargava, B. N., N. S. Sastri, B. R. Arora, and R. Rajaram, The afternoon counter-electrojet phenomenon, Ann. Geophys., 36, 231-240, 1980.

Butcher, E. C., An investigation of the causes of abnormal quiet days in Sq (H), Geophys. J. R. astr. Soc., 69, 101-111, 1982.

Butcher, E. C., and G. M. Brown, Abnormal quiet days and the effect of the interplanetary magnetic field on the apparent position of the Sq focus, Geophys. J. R. astr. Soc., 63, 783-789, 1980.

Butcher, E. C. and G. M. Brown, On the nature of abnormal quiet days in Sq (H), Geophys. J. R. astr. Soc., 64, 513-526, 1981a.

Butcher, E. C., and G. M. Brown, The variability of Sq (H) on normal quiet days, Geophys. J. R. astr. Soc., 64, 527-537, 1981b.

Davis, T. N., K. Burrows, and J. D. Stolarik, A latitude survey of the equatorial electrojet with rocket-borne magnetometers, J. Geophys. Res., 72, 1845-1861, 1967.

Egedal, J., Daily variation of the horizontal magnetic force at the magnetic equator, Nature, 161, 443-444, 1948.

Fejer, B. G., D. T. Farley, R. F. Woodman, and C. Calderon, Dependence of equatorial F region vertical drifts on season and solar cycle, J. Geophys. Res., 84, 5792-5796, 1979.

Feldstein, Y. I., R. G. Afonina, B. A. Belov, and A. E. Levitin, Magnetic field and field-aligned current variations in the polar cusp controlled by interplanetary medium parameters, Planet. Space Sci., 30, 635-640, 1982.

Forbes, J. M., and R. S. Lindzen, Atmospheric solar tides and their electromagnetic effects, I, The global Sq current system, J. Atmos. Terr. Phys., 38, 897-910, 1976a.

Forbes, J. M., and R. S. Lindzen, Atmospheric solar tides and their electromagnetic effects, II, The equatorial electrojet, J. Atmos. Terr. Phys., 38, 911-920, 1976b.

Fukushima, N., Electric potential difference between conjugate points in middle latitudes caused by asymmetric dynamo in the ionosphere, J. Geomagn. Geoelect., 31, 401-409, 1979.

Gagnepain, J., N. Crochet, and A. D. Richmond, Theory of longitudinal gradients in the equatorial electrojet, J. Atmos. Terr. Phys., 38, 279-286, 1976.

Graham, G., An account of observations made of variation of the horizontal needle at London, in the latter part of the year 1722, and beginning of 1723, Philos. Trans. R. Soc. London, 383, 96-107, 1724.

Heelis, R. A., P. C. Kendall, R. J. Moffett, D. W. Windle, and H. Rishbeth, Electrical coupling of the E- and F- regions and its effect on F-region drifts and winds, Planet. Space Sci., 22, 743-756, 1974.

Iijima, T., and T. A. Potemra, The amplitude distribution of field-aligned currents at northern high latitudes observed by TRIAD, J. Geophys. Res., 81, 2165-2174, 1976.

Iijima, T., and T. A. Potemra, Large scale characteristics of field-aligned currents associated with substrom, J. Geophys. Res., 83, 599-615, 1978.

Iwasaki, N. and A. Nishida, Ionospheric current system produced by an external electric field in the polar cap, Rep. Ionos. Space Res. Japan, 21, 17-28, 1967.

Kamide, Y., and S. Matsushita, Simulation studies of ionospheric electric fields and currents in relation to field-aligned currents, 1, Quiet periods, J.Geophys. Res., 84, 4083-4098, 1979a.

Kamide, Y., and S. Matsushita, Simulation studies of ionospheric electric fields and currents in relation to field-aligned currents, 2, Substorms, J. Geophys. Res., 84, 4099-4115, 1979b.

Kamide, Y., A. D. Richmond, and S. Matsushita, Estimation of ionospheric electric fields, ionospheric currents, and field-aligned currents from ground magnetic records, J. Geophys. Res., 86, 801-813, 1981.

Kato, S., Horizontal wind systems in the ionospheric E region deduced from the dynamo theory of geomagnetic Sq variation, IV, J. Geomagn. Geoelect., 8, 24-37, 1956.

King-Hele, D. G., and D. M. C. Walker, Upper-atmosphere zonal winds. Variation with height and local time, Planet. Space Sci., 25, 313-336, 1977.

Maeda, H., Horizontal wind systems in the ionospheric E region deduced from the dynamo theory of the geomagnetic Sq variation, I, Non-rotating earth, J. Geomagn. Geoelect., 7, 121-132, 1955.

Maeda, H., Horizontal wind systems in the ionospheric E region deduced from the dynamo theory of the geomagnetic Sq variation, III, J. Geomagn. Geoelect., 9, 86-93, 1957.

Maeda, H., Field-aligned current induced by asymmetric dynamo action in the ionosphere, J. Atmos. Terr. Phys., 36, 1395-1401, 1974.

Maeda, H., and K. Maekawa, A numerical study of polar ionospheric current, Planet. Space Sci., 21, 1287-1300, 1973.

Maeda, H., and H. Murata, Electric currents induced by nonperiodic winds in the ionosphere, 1, J. Geophys. Res., 73, 1077-1092, 1968.

Maeda, H., T. Iyemori, T. Araki, and T. Kamei, New evidence of a meridional current system in the equatorial ionosphere, Geophys. Res. Lett., 9, 337-340, 1982.

Maekawa, K., Global distribution of electric fields and currents in the ionosphere produced by field-aligned currents of magnetospheric origin, J. Atmos. Terr. Phys., 42, 673-682, 1980.

Maekawa K., and H. Maeda, Electric fields in the ionosphere produced by polar field-aligned currents, Nature, 273, 649-650, 1978.

Malin, S. R. C., Worldwide distribution of geomagnetic tides, Philos. Trans. R. Soc. London, A274, 551-594, 1973.

Maltsev, Y. P., S. V. Leontyev, and V. B. Lyatskiy, Electric fields and currents in the boundary region of electrojets, Geomag. Aeron., 14, 128-129, 1974.

Matsushita, S., Interaction between the ionosphere and the magnetosphere for Sq and L variations, Radio Sci., 6, 279-294, 1971.

Matsushita, S., and H. Maeda, On the geomagnetic solar quiet daily variation field during the IGY, J. Geophys. Res., 70, 2535-2558, 1965.

Matuura, N., Electric fields deduced from the thermospheric model, J. Geophys. Res., 79, 4679-4689, 1974.

Mayaud, P. N., The equatorial counter-electrojet, a review of its geomagnetic aspects, J. Atmos. Terr. Phys., 39, 1055-1070, 1977.

Mazaudier, C., Electric currents above St.-Santin, 1, Data, J. Geophys. Res., 87, 2459-2464, 1982.

Mazaudier, C., and M. Blanc, Electric currents above St.-Santin, 2, Model, J. Geophys. Res., 87, 2465-2480, 1982.

Musmann, G., and E. Seiler, Detection of meridional currents in the equatorial ionosphere, J. Geophys., 44, 357-372, 1978.

Raghavarao, R., and B. G. Anandarao, Vertical winds as a plausible cause for equatorial counter electrojet, Geophys. Res. Lett., 7, 357-360, 1980.

Rastogi, R. G., Counter equatorial electrojet currents in the Indian zone, Planet. Space Sci., 21, 1355-1365, 1973.

Rees, D., P. A. Rounce, G. T. Best, and A. F. Quesada, Midlatitude measurements of the thermospheric neutral winds during the ALLADDIN programme, J. Atmos. Terr. Phys., 41, 1171-1178, 1979.

Richmond, A. D., Equatorial electrojet, I, Development of a model including winds and instabilities, J. Atmos. Terr. Phys., 35, 1083-1103, 1973a.

Richmond, A. D., Equatorial electrojet, II, Use of the model to study the equatorial ionosphere, J. Atmos. Terr. Phys., 35, 1105-1118, 1973b.

Richmond, A. D., S. Matsushita, and J. D. Tarpley, On the production mechanism of electric currents and fields in the ionosphere, J. Geophys. Res., 81, 547-555, 1976.

Rishbeth, H., The F-layer dynamo, Planet. Space Sci., 19, 263-267, 1971a.

Rishbeth, H., Polarization fields produced by winds in the equatorial ionosphere, Planet Space Sci., 19, 357-369, 1971b.

Salah, J. E., and J. V. Evans, Tests of electrodynamic consistency from dayside ionospheric drift observations, J. Geophys. Res., 82, 2413-2418, 1977.

Stening, R. J., Calculation of electric currents in the ionosphere by an equivalent circuit method, Planet. Space Sci., 16, 717-728, 1968.

Stening, R. J., An assessment of the contribution of various tidal winds to the Sq current system, Planet. Space Sci., 17, 899-908, 1969.

Stening, R. J., Field-aligned currents driven by the ionospheric dynamo, J. Atmos. Terr. Phys., 39, 933-937, 1977a.

Stening, R. J., Magnetic variations at other latitudes during reverse equatorial electrojet, J. Atmos. Terr. Phys., 39, 1071-1077, 1977b.

Sugiura, M., and J. C. Cain, A model equatorial electrojet, J. Geophys. Res., 71, 1869-1877, 1966.

Sugiura, M., and D. J. Poros, An improved model equatorial electrojet with a meridional current system, J. Geophys. Res., 74, 4025-4034, 1969.

Suzuki, A., UT and day-to-day variations in equivalent current systems for world geomagnetic variations, J. Geomagn. Geoelect., 31, 21-46, 1979.

Takeda, M., and H. Maeda, Equivalent Sq current system at occasions of equatorial counter electrojet, J. Geomagn. Geoelect., 32, 297-301, 1980.

Takeda, M., and H. Maeda, F-region dynamo in the evening, submitted to J. Atmos. Terr. Phys., 1983.

Tarpley, J. D., The ionospheric wind dynamo, I, Lunar tide, Planet. Space Sci., 18, 1075-1090, 1970a.

Tarpley, J. D., The ionospheric wind dynamo, II, Solar tide, Planet. Space Sci., 18, 1091-1103, 1970b.

Untiedt, J., A model of the equatorial electrojet involving meridional currents, J. Geophys. Res., 72, 5799-5810, 1967.

Van Sabben, D., Ionospheric current systems caused by non-periodic winds, J. Atmos. Terr. Phys., 24, 959-974, 1962.

Van Sabben, D., The computations of magnetospheric currents caused by dynamo action in the ionosphere, J. Atmos. Terr. Phys., 31, 469-474, 1969.

Van Sabben, D., Solstitial Sq-currents through the magnetosphere, J. Atmos. Terr. Phys., 32, 1331-1336, 1970.

Volland, H., and L. Grellmann, A hydromagnetic dynamo of the atmosphere, J. Geophys. Res., 83, 3699-3708, 1978.

Woodman, R. F., Vertical drift velocities and east-west electric fields at the magnetic equator, J. Geophys. Res., 75, 6249-6259, 1970.

Woodman, R. F., R. G. Rastogi, and C. Calderon, Solar cycle effects on the electric fields in the equatorial ionosphere, J. Geophys. Res., 82, 5257-5261, 1977.

Yasuhara, F., and S.-I. Akasofu, Field-aligned currents and ionospheric electric fields, J. Geophys. Res., 82, 1279-1284, 1977.

Yasuhara, F., Y. Kamide, and S.-I. Akasofu, Field-aligned currents and ionospheric currents, Planet. Space Sci., 23, 1355-1368, 1975.

Zmuda, A. J., J. H. Martin, and F. T. Heuring, Transverse magnetic disturbances at 1100 km in the auroral region, J. Geophys. Res., 71, 5033-5045, 1966.

Zmuda, A. J., J. H. Heuring, and J. H. Martin, Daytime magnetic disturbances at 1100 km in the auroral oval, J. Geophys. Res., 72, 1115-1117, 1967.